Working paper

2022-08

Statistics and Econometrics
ISSN 2387-0303

Spatial extreme model for rainfall intensity.
Application to the estimation of IDF curves in the Basque Country

Roberto Mínguez, Sixto Herrera

uc3m | Universidad Carlos III de Madrid

Spatial extreme model for rainfall intensity

Application to the estimation of IDF curves in the Basque Country

Mínguez R.[1*] and Herrera S.[2]

[1*]Department of Statistics, Universidad Carlos III de Madrid, Leganés, Madrid, Spain.
[2]Applied Mathematics and Computer Science Department, Universidad de Cantabria, Santander, Cantabria, Spain.

*Corresponding author(s). E-mail(s): rminguez@est-econ.uc3m.es;
Contributing authors: sixto.herrera@unican.es;

Abstract

Intensity-duration-frequency (IDF) curves are commonly used in engineering practice for the hydraulic design of flood protection infrastructures and flood risk management. IDF curves are simple functions between the rainfall intensity, the timescale at which the rainfall process is studied, and the return period. This work proposes and tests a new methodological framework for the spatial analysis of extreme rainfall intensities at different time scales, taking advantage of two different precipitation datasets: local observational and gridded products. On the one hand, the proposed method overcomes or reduces known issues related to observational datasets (missing data and short temporal coverage, outliers, systematic biases and inhomogeneities, etc.). On the other hand, it allows incorporating appropriately terrain dependencies on the spatial distribution of the extreme precipitation regime. Finally, it allows to estimate the IDF curves at regional level in contrast with the local approach only based on rain gauges commonly used in practice. The method has been tested to compute IDF curves all over the Basque Country, contrasting results with respect to local analyses. Results show the method robustness against outliers, missing data, systematic biases and short length time series. Moreover, since GEV-parameters from daily gridded dataset are used as covariates, the

proposed approach allows coherent spatial interpolation/extrapolation of IDF curves properly accounting for the influence of orographic factors. In addition, due to the current coexistence of local observations and gridded datasets at regional (e.g. The Alps), national (e.g. Spain, France, etc.) or international scale (e.g. E-OBS for Europe or Daymet for the United States of America), the proposed methodology has a wide range of applicability in order to fulfill the known gaps of the observational datasets and reduce the uncertainty related with analysis and characterization of the extreme precipitation regime.

Keywords: precipitation extremes, return values, IDF curves

1 Introduction

Intensity-duration-frequency (IDF) curves are probably one of the most commonly used tools in engineering practice, which are very useful for the hydraulic design of flood protection infrastructures and flood risk management in general, having a great variety of applications (Grimaldi et al, 2011). IDF curves are simple functions between the rainfall intensity, the timescale at which the rainfall process is studied, and the return period. For more information about IDF curves, we recommend the state-of-the-art review by Salas et al (2020) related to probable maximum precipitation (PMP), closely related topic to IDF curves.

This practical interest has encouraged water management administrations to display rain gauges over the watersheds they manage to measure the amount of water that has fallen in real-time, which provide average rainfall intensities during time intervals of 10/15 minutes. These records allow the construction of IDF curves for different time scales, which should be updated from time-to-time to include the additional information gathered over time, and/or new methodological developments.

However, a common shortcoming of these datasets is that they do not usually have long enough records all over the area of interest to make return period estimates with confidence. As a result, most IDF curve adjustments are based on daily datasets with longer series (see Yan et al, 2021, and references therein). In addition, fitted IDF curves at locations where rain gauges are available provide local information about the extreme precipitation regime, which can not be easily extrapolated to the rest of the target region. In order to solve the spatial coverage problem of the observational networks and due to the known problems of these datasets (missing data, outliers, inhomogeneities due to instrumental and/or location changes, etc.) (Klein Tank et al, 2002; Herrera et al, 2012, 2019a) a commonly used approach is to build *gridded* ("regionalized" or "interpolated") datasets based on quality controlled observational networks, which cover long time periods and the region analyzed. In recent years, many gridded datasets have been developed at regional (Frei

and Schär, 1998; Bedia et al, 2013; Artetxe et al, 2019), national (Yatagai et al, 2007; Belo-Pereira et al, 2011; Herrera et al, 2012, 2019a), continental (Haylock et al, 2008; Thornton et al, 2020) and/or global (Lange, 2016, 2019; Dirk N. Karger et al, 2021) scale based on different interpolation approaches. Despite the known limitations of the interpolated datasets to reproduce the observed extreme values (Klok and Klein Tank, 2009; Herrera et al, 2012, 2019a), in general they are able to properly described the spatial dependencies of the variable and, depending on the stations density (Hofstra et al, 2010; Herrera et al, 2019b), the influence on the rainfall distribution of orographic factors, such as elevation, distance from shoreline, blockages, exposures, curvatures, etc. Based on the advantages and shortcomings of both types of rainfall datasets a question appears: could a gridded dataset be used as a complement of rain gauges for the IDF-curve estimation problem?

In this sense, the combination of different datasets for extreme value analysis is not new. Extreme mixed models have been used to combine reanalysis and instrumental data. Mínguez et al (2013) proposes the mixed extreme value (MEV) climate model for wave analysis. This method allows correcting discrepancies between instrumental and reanalysis records in the upper tail and it is consistent with extreme value theory. However, in order to characterize stochastically the differences between instrumental and reanalysis maxima, it only uses information about annual maxima. In Mínguez and Del Jésus (2015) the method is extended to be applied with alternative models such as Pareto-Poisson (Leadbetter et al, 1983) or Peaks Over Threshold (POT, Davidson and Smith (1990)), which are known to be more robust because they use more information during the estimation process.

In addition, recent advances in the extreme value theory (see Coles (2001); Katz et al (2002) as general references) allow modeling the natural variability of extreme events of environmental and geophysical variables based on regression models. These methods introduce time-dependent variations within a certain time scale (year, season or month) and the possibility to construct regression models to show how the variables of interest may depend on other measured covariates. Examples of these kinds of models can be found in Carter and Challenor (1981), which proposes a month-to-month distribution assuming that data are identically distributed within a given month. Smith and Shively (1995) constructed a regression model for the frequency of high-level ozone exceedances in which time and meteorology are regressors. Morton et al (1997) apply a seasonal POT model to wind and significant wave height data. Analogous models but applied to different geophysical variables can be found in Coles (2001), Katz et al (2002) or Méndez et al (2007). Méndez et al (2006) developed a time-dependent POT model for extreme significant wave height which considers the parameters of the distribution as functions of time (harmonics within a year, exponential long-term trend, the Southern Oscillation Index (SOI), etc.). Brown et al (2008) studied the global changes in extreme daily temperature since 1950 considering possible trends and the influence of the North Atlantic Oscillation (NAO). Menéndez et al (2009) and

Izaguirre et al (2010) developed a time-dependent model based on the Generalized Extreme Value (GEV) distribution that accounts for seasonality and interannual variability of extreme monthly significant wave height. Northrop (2004) proposes a regression model to describe a region-of-influence approach for flood frequency analysis.

The motivation of this work comes, firstly, from the effort that the Basque Country's Government has made in recent years to improve the knowledge about the climate and water resources of the region, and secondly, from the purpose to take full advantage of all climatic information available all over the Basque Country, which includes instrumental rain gauges of high temporal frequency (see Fig. 1) and a high spatial resolution gridded dataset of daily precipitation (Artetxe et al, 2019). In addition, the Basque Water Agency (Uraren Euskal Agentzia) has promoted and carried out many hydrological and meteorological studies in order to define the average annual rainfall and the regime of extremes, however most of these studies have not collected IDF curves, information of interest to many administrations and individuals, and in those locations where IDF curves have been defined, they have become obsolete and, therefore, it is necessary to update them.

In summary, the aim of this work is to take advantage of the precipitation datasets available for the Basque Country to present a new methodological framework for the spatial analysis of extreme rainfall intensities at different time scales with the following features:

1. Being robust with respect to abnormally high records (outliers). Given the number of available rain gauges, it is advisable to have a methodology that is not sensitive to these anomalous data.
2. Being robust in case the data provided by a rain gauge contains systematic biases due to location, exposure to wind and/or obstacles, among other causes.
3. Being robust with respect to the existence of gaps in time series enabling not to discard records of incomplete years with a high percentage of gaps in the series.
4. Make it robust with respect to the length of the series. There is no doubt that the longer the record, the lower the uncertainty in return period estimations. It would be convenient to have a method that gives more weight to long records than to short ones, without the need to discard short ones from the analysis. Note that it is recognized in the technical literature that when using short records, there is a lack of information on large hydrological events, which is one of main drawbacks in flood frequency analysis and there is a need of "temporal information expansion," to obtain reliable enough results concerning quantiles of large return periods (Salas et al, 2020).
5. Allowing coherent spatial interpolation/extrapolation, i.e. taking into account the influence of orographic factors such as elevation, distance from shoreline, blockages, exposures, curvatures, etc.

In order to achieve these goals, in this paper we propose the combination of instrumental data given by rain gauges and the tail information given by the high-resolution daily precipitation gridded dataset over the Basque Country. We characterise the tail of intensity rainfall for different timescales from instrumental records and using the tail behavior of daily precipitations as covariates. Those covariates allows us to interpolate/extrapolate the tail of intensity rainfall for different timescales all over the gridded domain. It is precisely in those covariates where the influence of orographic factors such as elevation, distance from shoreline, blockages, exposures, curvatures, etc. is gathered.

Note that the current availability of daily precipitation gridded datasets makes the proposed method highly applicable to make a coherent and robust spatial analysis of extreme intensity rainfall for different timescales, i.e. to make IDF curves. In addition, the positive features of the method and its robustness might justify the effort of developing specific high resolution daily precipitation gridded data sets prior making any extreme value analysis of intensity rainfall.

The rest of the manuscript is organized as follows. Section 2 presents the observational (2.1) and gridded datasets (2.2) used, and the proposed extreme value analysis model (2.3). Section 3 shows the performance on real data from Basque Country. Finally, in Section 4 relevant conclusions are drawn.

2 Data and Methods

In this section, firstly, the observational precipitation data and the gridded dataset are described, including the interpolation method used to build the high resolution daily precipitation gridded dataset for the Basque Country, and secondly, the spatial extreme value model is described in detail.

2.1 Basque Water Agency Rain Gauges

Figure 1 shows the observational network deployed by the Basque Water Agency (Uraren Euskal Agentzia) covering the different watersheds of the region. This dataset is composed by 131 rain gauges distributed all over the Basque Country covering the period 1989-2020 (see Appendix A for a detailed description of the stations network). The average precipitation amount is registered at 10- and 15-minute time intervals, obtaining the values at different timescales (30, 60, 120, 180, 240, 360, 720 and 1440 minutes) by aggregating the corresponding 10- or 15-minute values using a rolling window.

Note that, despite the large number of rain gauges available, in previous analyses many stations were discarded due to:

1. uncertainties associated with the measurements,
2. the differences in measurement technology among rain gauges, and
3. the disparity in record lengths.

Moreover, precipitation records were brushed up before its use, checking for missing values and outliers. In this sense, filtering anomalous data when

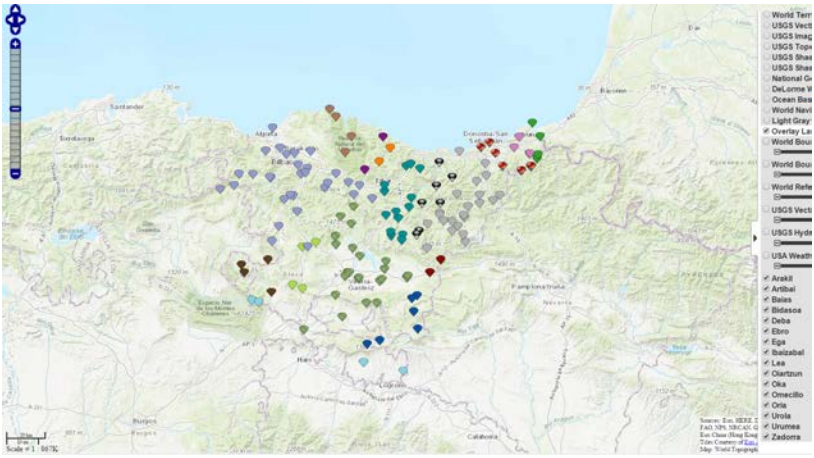

Fig. 1 Rain gauges locations all over the Basque Country. Each type of marker is associated with a different watershed.

dealing with the right tail is complex if you do not have clear indicators that there might be an inconsistency in the data.

An important issue for any extreme value analysis is the record length. In this particular case, the vast majority of the records are more than 5 years old as shown in Figure 2. The standards of good practice advise not to perform extreme analyzes with less than 10 years of data, however we have set out 5 years as minimum length used in this analysis, disregarding those with lower record length. There are two reasons: a) the minimum of ten years can be slightly reduced in case of using the peaks-over-threshold approach, and b) one of the aims of the manuscript is to show how the proposed method allows not to disregard short record lengths from the analysis.

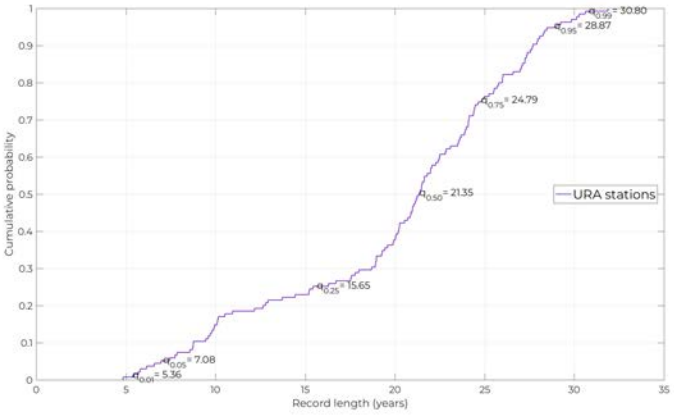

Fig. 2 Cumulative distribution function of record lengths associated with rain gauges in the Basque Country.

2.2 Daily precipitation gridded dataset

In the framework of the https://www.euskadi.eus/web01-a2ingkli/es/contenidos/documentacion/klima2050/en_def/index.shtml a high spatial resolution (1 km^2) gridded dataset for daily precipitation and mean, maximum and minimum daily temperatures was developed covering the period 1971-2016, which was updated until 2019 for this study, by applying the methodology proposed in Artetxe et al (2019).

This grid was developed considering a quality controlled observational dataset that combines stations belonging to the Spanish National Weather Service (AEMET), the Basque Weather Service (EuskalMet) and the Basque Water Agency (URA - Uraren Euskal Agentzia). Only stations with at least 20 consecutive years with at least the 80% of the data were included in the final dataset. In the case of the EuskalMet and URA stations, due to the shorter time coverage, the threshold was reduced to at least 10 years. In addition, stations with less than the 50% of the monthly time series, considering for each month the same 80% threshold of data available, were removed of the final dataset. In addition, precipitation outliers were identified considering as threshold 4 times the 90th percentile of the rainy days and removed from the time series. As a result, the final dataset considered for the interpolation contained 244 (164) stations for precipitation (temperature) (see Fig. 3 in Artetxe et al, 2019).

In order to reach the final resolution a three–step regression-kriging (Hengl et al, 2007) interpolation process was conducted:

- First, the monthly rainfall values were obtained by regression considering as regressors a set of basic covariates describing terrain characteristics including elevation, distance to coastline, and topographic blocking effects.
- Secondly, the monthly residual obtained with the regression model was interpolated with ordinary kriging and added to the monthly value obtained with the regression model.
- Finally, the daily anomaly was obtained by applying ordinary kriging (Atkinson and Lloyd, 1998; Biau et al, 1999; Haylock et al, 2008; Herrera et al, 2012) to the regression residuals. Both the daily anomaly and the monthly values are combined to obtain the final daily estimations.

The high-resolution orography was obtained from the digital elevation model https://lta.cr.usgs.gov/GTOPO30 (Gesch et al, 1999) with an spatial resolution of 30" which corresponds to $1km$ at these latitudes.

Note that the monthly value for precipitation corresponds to the total precipitation amount for that month and, thus, the daily anomaly is defined as the quotient between the daily precipitation value and the total monthly precipitation amount. As a result, the daily value is obtained by multiplying the estimated monthly values and the daily anomalies.

The final result constitutes a high-resolution gridded dataset of daily values of precipitation all over the Basque Country, including the main topographic

dependencies given by the observations due to the regression model used in the interpolation process.

2.3 Spatial extreme value analysis model

Before describing the proposed spatial extreme value analysis model for intensity rainfall, we provide some insights about extreme value distributions (Castillo, 1988; Castillo et al, 2005, 2008) required to understand where our model comes from.

2.3.1 Extreme value analysis models

Given any random variable X, the distribution of the maximum of a sample of size n drawn from a population with *cumulative probability distribution* (CDF) $F_X(x)$, assuming independent observations, corresponds to $F_X(x)^n$. However this result does not tell us anything for large samples, i.e. when $n \to \infty$, because:

$$\lim_{n\to\infty} F_X(x)^n = \begin{cases} 1 \text{ if } F_X(x) = 1 \\ 0 \text{ if } F_X(x) < 0 \end{cases} \tag{1}$$

To avoid degeneracy, a linear transformation is looked for such that:

$$\lim_{n\to\infty} F_X(a_n + b_n x)^n = H(x); \ \ \forall x \tag{2}$$

are not degenerate, where a_n and b_n are constants, which depend on n.

It turns out (Fisher and Tippett (1928); Tiago de Oliveira (1958); Galambos (1987)) that only one parametric family satisfies (2) and it is known as *generalized extreme value* (GEV) distribution with CDF given by:

$$H(x;\ \mu,\psi,\xi) = \begin{cases} \exp\left\{-\left[1+\xi\left(\dfrac{x-\mu}{\psi}\right)\right]_+^{-\frac{1}{\xi}}\right\}; \ \xi \neq 0, \\ \exp\left\{-\exp\left[-\left(\dfrac{x-\mu}{\psi}\right)\right]\right\}; \ \begin{matrix} -\infty < x < \infty \\ \xi = 0 \end{matrix} \end{cases},$$

where $[a]_+ = \max(0, a)$, μ, ψ, ξ are the location, scale and shape parameters, respectively, and the support is $x \leq \mu - \psi/\xi$ if $\xi < 0$, $x \geq \mu - \psi/\xi$ if $\xi > 0$, or $-\infty < x < \infty$ if $\xi = 0$. The GEV distribution includes three distribution families corresponding to the different types of the tail behavior: Gumbel family ($\xi = 0$) with a light tail decaying exponentially; Fréchet distribution ($\xi > 0$) with a heavy tail decaying polinomially; and Weibull family ($\xi < 0$) with a bounded tail.

Distribution (3) is useful for analysing maximum rainfall intensity for different time scales if annual maxima series (AMS) are considered. The main problem with respect to AMS is that many records belonging to the right tail of the distribution are discarded. That is the reason why we rather using

the Peaks Over Threshold method (POT) (Davidson and Smith, 1990). The basic idea is that high exceedances occur in clusters associated with single storms. By separating out the peaks within those clusters, they will be approximately independent and can be fitted using the Poisson-Generalized Pareto Distribution (GPD) model. The latter relies on the following assumptions:

1. The number of independent storm peaks N exceeding threshold u in any one year follows a Poisson distribution with parameter λ.
2. The random variable X associated with independent storm peaks above the threshold u follows a Pareto distribution with cumulative distribution function:

$$G(x-u;\,\sigma,\xi)=\begin{cases}1-\left[1+\xi\left(\dfrac{x-u}{\sigma}\right)\right]_{+}^{-\frac{1}{\xi}}\;;\;\xi\neq 0,\\[2ex] 1-\exp\left[-\left(\dfrac{x-u}{\sigma}\right)\right];\quad \begin{matrix}-\infty<x<\infty\\ \xi=0\end{matrix},\end{cases}$$

where $[a]_+ = \max(0,a)$, σ,ξ are the scale and shape parameters, respectively, and the support is $u < x \leq u+\sigma/|\xi|$ if $\xi<0$, $x\geq u$ if $\xi>0$, or $u<x<\infty$ if $\xi=0$. The GPD distribution also includes three distribution families corresponding to the different types of the tail behavior: Exponential family ($\xi=0$); Pareto tail distribution ($\xi>0$); and one analogous to the Weibull family ($\xi<0$) and a bounded tail.

Supposing that $x > u$, this model allows to derive the cumulative distribution function of annual maxima as follows:

$$\begin{aligned}\text{Prob}\left(\max_{1\leq i\leq N} X_i \leq x\right) &= \text{Prob}(N=0)+\sum_{n=1}^{\infty}\text{Prob}(N=n)G(x-u)^n\\ &= e^{-\lambda}+\left[\sum_{n=1}^{\infty}\frac{e^{-\lambda}\lambda^n}{n!}G(x-u)^n\right] = e^{-\lambda\left[1+\xi\left(\frac{x-u}{\sigma}\right)\right]^{\frac{1}{\xi}}}.\end{aligned} \tag{3}$$

Considering the asymptotic relationship between return period (T) and annual maxima given by Beran and Nozdryn-Plotnicki (1977):

$$T=-\frac{1}{\log\left(\text{Prob}\left[\max_{1\leq i\leq N} X_i \leq x\right]\right)}, \tag{4}$$

the following relationship between Pareto-Poisson model and return period is derived:

$$T=\frac{1}{\lambda(1-G(x-u))}. \tag{5}$$

Conversely, quantile x_T associated with given return period T is obtained by solving the following implicit equation:

$$G(x_T - u) = 1 - \frac{1}{\lambda T}. \tag{6}$$

An advantage of this model is that it is entirely consistent with GEV. In fact expression (3) is equal to (3) if:

$$\sigma = \psi + \xi(u - \mu), \lambda = \left[1 + \xi\left(\frac{u-\mu}{\sigma}\right)\right]^{-\frac{1}{\xi}}. \tag{7}$$

Remark 1 We encourage using Poisson-GPD model because it allows taking more than one data for each year if more than one exceedances are present, and disregard those years whose maximum can be much below several order statistics with respect to other years. Besides, contrary to the thought that POT values converge to GPD given that the threshold tends to infinity (Salas et al, 2020), they do converge given that the threshold tends to the upper end of the random variable, which must be limited by physical considerations Castillo et al (2008).

2.3.2 Spatial model

A common practice in modern statistics is building regression models to show how the variable of interest may depend on other covariates. It is usual to include covariates in the location, scale and shape parameters associated with temporal variation such as in Mínguez et al (2010); Izaguirre et al (2012); Yan et al (2021). However, it is also possible to include covariates linked to geographic locations. In this specific case, the spatial model we propose has the following parameterization of the location, scale and shape parameters associated with the k-th element of the same spatial grid used for the daily precipitation regionalized dataset:

$$\mu_k = \beta_0 + \beta_1 \mu_k^d \tag{8}$$

$$\log(\psi_k) = \alpha_0 + \alpha_1 \log(\psi_k^d) \tag{9}$$

$$\xi_k = \gamma_0 + \gamma_1 \xi_k^d, \tag{10}$$

where parameters μ_k^d, ψ_k^d and ξ_k^d are the location, scale and shape parameters of the annual maximum distribution associated with daily precipitation records for k-th element of the spatial grid. Even though the model is described in terms of GEV parameters, we recommend using the POT method explained in the previous section for fitting both the spatial and the local models. GEV parameters can be obtained afterwards using expression (7).

2.3.3 Maximum likelihood estimation

For parameter statistical inference the method of maximum likelihood is used, maximizing the following log-likelihood function:

$$\ell(\boldsymbol{x}_k;\ \ k=1,\ldots,n_r,\boldsymbol{\theta}) = \sum_{k=1}^{n_r}\sum_{i=1}^{n_k} \log\left(\frac{dH(x;\ \mu_k,\psi_k,\xi_k)}{dx}\bigg|_{x=x_i^k} \right) \tag{11}$$

where $\boldsymbol{x}_k;\ \ k=1,\ldots,n_r$ is the set of intensity rainfall records for any timescale associated with peaks over threshold at rain gauge k, being n_r the number of rain gauges available, and x_i^k the i-th element of the corresponding record. $\boldsymbol{\theta}$ is the set of parameters to be estimated, i.e. $\boldsymbol{\theta} \in \{\beta_0,\beta_1,\alpha_0,\alpha_1,\gamma_0,\gamma_1\}$. Note that the log-likelihood function is composed by the log-likelihood functions for each rain gauge location, i.e. we perform a unique parameter estimation process for the spatial model, which contrast with the traditional individual fitting process usually performed in this type of analyses.

If we expand the log-likelihood function (11) using the relationship between GEV and Poisson-GPD models, it becomes:

$$\ell(\boldsymbol{x}_k;\ \ \forall k,\boldsymbol{\theta}) = \sum_{k=1}^{n_r} \begin{cases} \{n_k\log(\lambda_k) - T_k\lambda_k - n_k\log(\sigma_k) \\ \quad - \left[\left(1+\frac{1}{\xi_k}\right)\sum_{i=1}^{n_k}\log\left(1+\xi_k\frac{x_i^k-u_k}{\sigma_k}\right)\right]\} & \text{if } \xi_k \neq 0 \\ n_k\log(\lambda_k) - T_k\lambda_k - n_k\log(\sigma_k) - \sum_{i=1}^{n_k}\left(\frac{x_i^k-u_k}{\sigma_k}\right) & \text{if } \xi_k = 0 \end{cases} \tag{12}$$

where GPD-scale and Poisson parameters in terms of GEV parameters correspond to:

$$\left.\begin{aligned} \sigma_k &= \psi_k + \xi_k(u_k-\mu_k) \\ \lambda_k &= \left[1+\xi_k\left(\frac{u_k-\mu_k}{\sigma_k}\right)\right]^{-\frac{1}{\xi_k}} && \text{if } \xi_k \neq 0 \\ \lambda_k &= \exp\left(-\frac{u_k-\mu_k}{\sigma_k}\right) && \text{if } \xi_k = 0, \end{aligned}\right\};\ \forall k, \tag{13}$$

which could be substituted in (12) to express the log-likelihood function as a function of GEV location (μ_k), scale (ψ_k) and shape (ξ_k) parameters. Finally, expressions (8)-(10) allows to express the log-likelihood function as a function of model parameters $\boldsymbol{\theta} \in \{\beta_0,\beta_1,\alpha_0,\alpha_1,\gamma_0,\gamma_1\}$. Note that we estimate both GEV parameters and the regression parameters simultaneously for the whole region through the optimization of the likelihood function.

The maximization of the log-likelihood function can be done using an unconstrained nonlinear optimization routine, or even a constrained optimization method including upper and lower bounds for some parameters could be

used. In this particular application we used a Trust Region Reflective Algorithm under Matlab (MATLAB, 2018) with upper and lower bounds through the function `fmincon`. For details about the method see Coleman and Li (1994) and Coleman and Li (1996). The trust region reflective algorithm has been chosen because i) analytical first order derivative information can be included and ii) upper and lower bounds on parameters can be considered easily. Note that although the MLE parameter fitting is an unconstrained maximization problem, we rather use a constrained optimization solver to include parameter bounds, which makes the estimation more robust. All *Newton-type* routines require the user to supply starting values. However, the importance of good starting values can be overemphasized and, in this case, simple guesses are enough (Smith, 2001).

2.3.4 Automatic regression model selection based on sensitivity analysis

Parameterizations like (8)-(10) allow constructing complex models that better capture the characteristics of the extreme tail behavior related to rain intensity for different timescales. However, in order to avoid over fitting, we have to establish a compromise between obtaining a good fit and keeping the model as simple as possible (Akaike, 1973; Schwarz, 1978; Hurvich and Tsai, 1989; George and Foster, 1994). In this particular case, we use the method proposed in Mínguez et al (2010), a pseudo-steepest descent algorithm, which at every iteration and based on sensitivity analysis (first and second-order derivative) information, selects the best parameter to be introduced in the model that maximizes the increment in the log-likelihood function, which in this case is the parameter whose score test statistic absolute value is maximum. The algorithm continues including new parameters until the likelihood ratio test rejects the inclusion of new parameters.

Let us assume $\hat{\boldsymbol{\theta}}^{(j)}$ be the optimal maximum likelihood estimation of a subset from $\boldsymbol{\theta} \in \{\beta_0, \beta_1, \alpha_0, \alpha_1, \gamma_0, \gamma_1\}$ at iteration j, being $\ell^{(j)}\left(\hat{\boldsymbol{\theta}}^{(j)}\right)$ the optimal log-likelihood function value. The iterative process continues as follows:

Step 1: Set new values for parameter vector $\boldsymbol{\theta}$, such that,

$$\theta_i = \begin{cases} \hat{\theta}_i^{(j)} & \text{if } \theta_i \in \boldsymbol{\theta}^{(j)} \\ 0 & \text{otherwise} \end{cases} \tag{14}$$

Step 2: Compute for each parameter θ_i the corresponding score test statistic absolute value as follows;

$$S(\theta_i) = \frac{U(\theta_i)^2}{\mathcal{I}_{ii}}, \tag{15}$$

where $U(\theta_i)$ is the score (the derivative of the log-likelihood function) associated with parameter θ_i, and and $\mathcal{I}_{ii}$ is the corresponding diagonal element of the the observed Fisher information matrix, i.e. the negative of the log-likelihood Hessian matrix. We use the score test statistic as selection criterion

because in order to compare the different sets of parameters, they should be divided by the square root of their variance so that, for each parameters set, its square has expectation 1 under the null hypothesis. The score test statistic has this property, i.e. is properly scaled. Thus, the parameter with maximum score test statistic is considered the most influential parameter and it is the one chosen for the next iteration. Derivatives and hessian required to compute (15) can be obtained numerically by finite differences.

Step 3: The next set of parameters $\boldsymbol{\theta}^{(j+1)}$ results from the union between set $\boldsymbol{\theta}^{(j)}$ and parameter with maximum score test statistic:

$$\boldsymbol{\theta}^{(j+1)} = \boldsymbol{\theta}^{(j)} \cup \theta_i \Big| S(\theta_i) = \max_{\forall k} S(\theta_k). \tag{16}$$

Step 4: Compute the a new estimation of this new set of parameters $\hat{\boldsymbol{\theta}}^{(j+1)}$, being $\ell^{(j+1)}\left(\hat{\boldsymbol{\theta}}^{(j+1)}\right)$ the optimal log-likelihood function value. Note that a good starting point for the optimization routine is the vector $\boldsymbol{\theta}$ from (14).

[**Step 5:**] Compute the log-*likelihood ratio statistic* or *deviance* as follows:

$$T = 2\left\{\ell^{(j+1)}\left(\hat{\boldsymbol{\theta}}^{(j+1)}\right) - \ell^{(j)}\left(\hat{\boldsymbol{\theta}}^{(j)}\right)\right\}. \tag{17}$$

If the true model is given by the set of parameters $\hat{\boldsymbol{\theta}}^{(j)}$, the deviance follows a chi-square distribution with 1 degree of freedom (the difference in cardinality between the two sets). There are two possibilities:

1. If T is bigger than the upper-α point of the χ^2_1 distribution, the null hypothesis is rejected, being the proper model that given by $\hat{\boldsymbol{\theta}}^{(j+1)}$. Update the iteration counter $j \leftarrow j+1$ and go to **Step 1**.
2. If T is lower than or equal to the upper-α point of the χ^2_1 distribution, the null hypothesis is accepted. The proper model is that given by $\hat{\boldsymbol{\theta}}^{(j)}$. Stop the process.

Remark 2 Although we initially propose a purely based statistical method for parameter selection, we also recommend to follow the practical guidelines given by Castillo et al (2008), which encourages to disregard domains of attraction based on physical considerations. In this particular case, precipitation has a physical limit which allows us to disregard Frechet. In those cases where the proposed parameter selection method derives in a Frechet tail, we should reconsider and take Gumbel. Note that Frechet tail behaviour might be induced by the presence of a high return period within our data set.

2.3.5 Practical implementation

Once we have described the main ingredients of the method proposed, in this section we enumerate the required steps in order to analyse the rainfall

intensity for a given timescale or duration d. Prior to this analysis, it is required to fit the GEV model for each location associated with the high resolution daily gridded data set. We make this fitting using the maximum likelihood method for each point and we have at our disposal the location, scale and shape parameters (μ_k^d, ψ_k^d and ξ_k^d; $\forall k$) at each point of the grid. These are used as covariates for our spatial model. Next, the spatial fitting process is as follows:

1. Let assume we have at our disposal n_r time series of precipitation intensities at fixed temporal resolution t_0 at r different locations. Typical values are, for instance, $t_0 \in \{5, 10, 15\}$ minutes.
2. The number of elements in each time series might be different among them and equal to n_k^0; $k = 1, \ldots, r$. The total duration of each time series is equal to $T_k = t_0 n_k^0$; $k = 1, \ldots, r$.
3. Time series must be aggregated at the desired duration (d) using a moving window with length d/t_0. Note that these temporal series are highly temporally correlated, however, the selection procedure to determine the peaks over threshold will remove temporal autocorrelation for each series in the final data set.
4. For each time series a threshold u_k; $k = 1, \ldots, r$ must be selected, and then the peaks of clusters above the threshold are taken. We recommend to use a minimum distance in time criteria to ensure that peaks truly belong to independent storms. These data constitutes vectors $\boldsymbol{x}_k$; $k = 1, \ldots, r$ to be fitted. Note that criteria to select the appropriate thresholds are given in Davidson and Smith (1990).
5. Given the locations of data gauges, interpolate location, scale and shape parameters $\mu_k^d, \psi_k^d, \xi_k^d$; $k = 1, \ldots, r$ using the gridded parameters. The interpolation could be done using the nearest neighbour criteria, lineal, bilineal interpolation, or any other spatial interpolation method. It mostly depends on the spatial resolution and how gridded parameters change over space.
6. Next step is the automatic regression model selection explained in detail in section 2.3.4. We recommend start fitting the model using the set of parameters $\boldsymbol{\theta}^{(0)} = \{\beta_0, \alpha_0\}$, which corresponds to the same Gumbel distribution all over the rain gauge locations, and using as initial values for the optimization routine the mean and the logarithm of the standard deviation of all samples, respectively.
7. Once the optimal model and parameter values are achieved, the rainfall intensity distribution for a given timescale or duration d at any location inside the grid is available.

2.3.6 Leave-One-Out Cross-Validation (LOOCV)

To test the robustness of the proposed method, we also perform a leave-one-out cross-validation to compare the spatial model at each location where data is available. In this particular case, we fit a different spatial model at each

location by removing the data associated with the specific location. With this strategy we can estimate how good is the model performance in locations where we have no observations, which would give us a hint about how confidence and/or reliable we could be while using the spatial interpolation proposed by our model. Note that there is not any station in common between the Basque Water Agency rain gauges and the observational network used to build the gridded dataset, ensuring the independence needed in the any cross-validation approach.

2.3.7 Diagnostics

The model proposed in this paper is based on several assumptions. For this reason, once the parameter estimation process is completed, it is very important to make and run different diagnostic plots and statistical hypothesis tests to check whether the selected distributions might be considered appropriate or not.

- Cramer-von Mises and Anderson-Darling tests proposed by Chen and Balakrishnan (1995) to check at each location if the GPD fits (local and spatial) are acceptable. The null hypothesis (H_0) is that the exceedances at each location $\boldsymbol{x}_k - u_k$ follow the fitted Generalized Pareto distributions. If H_0 is not rejected then the original data is accepted to come from the GPD distribution.
- Sample autocorrelation and partial autocorrelation functions related to the transformed sample $\boldsymbol{z}_k^P$ coming from:

$$G(\boldsymbol{x}_k - u_k) = \Phi(\boldsymbol{z}_k^P); \quad k = 1, \ldots, n_p \tag{18}$$

  These functions help checking the independence assumption between peaks over threshold, whose values should be within the confidence bounds.
- To further explore the independence hypothesis, the Ljung-Box (Box and Pierce, 1970; Ljung and Box, 1978) lack-of-fit hypothesis test (Brockwell and Davis, 1991) for model misidentification is applied to the transformed sample $\boldsymbol{z}_k^P$. This test indicates the acceptance or not of the null hypothesis that the model fit is adequate (no serial correlation at the corresponding element of Lags).
- Cramer-von Mises and Anderson-Darling tests proposed by Chen and Balakrishnan (1995) to check at each location if the Poisson-GPD (using the GEV equivalence) fits (local and spatial) are acceptable. The null hypothesis (H_0) is that the annual maxima at each location $\boldsymbol{x}_k^{AMS}$ follow the fitted Generalized Extreme Value distributions. If H_0 is not rejected then the original data is accepted to come from the GEV distributions. Note that $\boldsymbol{x}_k^{AMS}$ correspond to the annual maxima series extracted from peaks over threshold.

3 Application to the estimation of IDF curves in the Basque Country

This section describes the application of the proposed method with the aim of constructing IDF curves all over the Basque Country based on the 131 rain gauges (see Figure 1) and the high resolution daily precipitation grid described in sections 2.1 and 2.2, respectively. To make the analysis, we follow the steps given in section 2.3.5.

3.1 Annual maxima daily rainfall fitting over the 1km of spatial resolution grid

The first step consists of analyzing the daily rainfall data from 1971 to 2019 over the grid of 1km of spatial resolution and fitting annual maxima to an extreme value distribution. Note that in this case we have 49 years of data, for this reason, we use the AMS method using the GEV as shown in the section 2.3.1. We have not used The Pareto-Poisson model because the threshold parameter must be selected carefully, and we have 12,389 points to be fitted, that is the reason to select AMS instead.

In addition, we check at every node of the grid if the shape parameter is statistically significant or not using the likelihood ratio test given in section 2.3.5, **step 5**.

We fitted 12,389 distributions, all of them Gumbel with null shape parameter, to all locations where data were available. Results associated with location (μ) and scale (ϕ) parameters are shown in Figures 3(a) and 3(b), respectively. Note that units correspond to millimeters of daily precipitation. These two graphs clearly point out how the orography (see Figure 4) affects the rainfall behaviour also at the tail of the distribution so, in order to include this driver in our model, we consider these quantities as spatial covariates in the **spatial** model.

3.2 Local and spatial extreme value analysis at rain gauge locations

Once the covariates are available for the spatial model, we proceed to the fitting process for different durations. We are going to consider the following timescales: 10, 20, 30, 60, 120, 180, 240, 360, 720 and 1440 minutes with the following considerations:

1. For the 10 and 20 minute timescales we only consider in the fitting process rain gauges with a ten minute record frequency.
2. For the rest of timescales, we used the data from all the rain gauges regardless of the recording frequency. However, we take into consideration each recording frequency for appropriate re-scaling.
3. For comparison purposes, besides the spatial analysis we also make local extreme value analysis.

Table 1 provides both local and spatial extreme value fitting information associated with analyzed rain gauges, in particular the following information is given:

1. Name of the rain gauge.
2. Poisson fitted parameter (λ) associated with Poisson-GPD model in events per year.
3. Scale parameter (σ) from GPD distribution of precipitation exceedances in mm.
4. Shape parameter (ξ).
5. Selected threshold (u) in mm.
6. Location (μ) and scale (ψ) parameters related to GEV annual maxima distribution.
7. p_{W}-values related to Cramer-von Mises test associated with GPD fitting. Note that we do not provide the Anderson-Darling test results in this table, however we compare both tests results in next subsections.
8. p_1, p_2, p_3, p_4-values associated with Ljung-Box lack-of-fit hypothesis test to check whether exceedances over the threshold are temporally independent.
9. $p_{\mathrm{W}}^{\max}$-values related to Cramer-von Mises test associated with GEV annual maxima fitting.

From these Tables the following considerations are in order:

1. Most of the local fitted distributions correspond to Gumbel, i.e. null shape parameter $\xi = 0$. However, there are 9 rain gauges (Berriatua, Aixola, Lastur Pluviometro, La Garbea, Mañaria, Orozko (Altube), Oiz, Muxika, Ereñozu) where local tail behaviour corresponds to Frechet $\xi > 0$, and 2 of them (Bidania, Estanda) correspond to Weibull $\xi < 0$ (bold faced shape parameter values). This contrasts with spatial fitted results, where all rain gauges correspond to Gumbel. Note that in those locations where the local tail is different from Gumbel either the length of the record is short or there exist a very large event which pushes the tail towards Frechet behaviour. This last effect is observed in Figure 5 for the fitting process associated with 1440 minutes timescale in Lastur (LAST), where the precipitation event above 200 mm pushes the local fitted tail towards Frechet, while the spatial fit is Gumbel.
2. p_W-values related to Cramer-von Mises test associated with GPD local and spatial fitting are simultaneously above significance level $\alpha = 0.05$ in all locations but in 10, being 9 out of 10 above 0.01 and the minimum equal to 0.007, i.e. the hypothesis of exceedances coming from Pareto distribution is rarely rejected. It is worth emphasizing that in Estanda the null hypothesis related to the local fitting is accepted (Weibull tail) but the one for spatial fitting (Gumbel tail) is rejected.
3. Regarding the independence assumption for peaks, most p-values from Ljung-Box lack-of-fit hypothesis test are above significance level $\alpha = 0.05$, i.e. independence assumption between peaks is also rarely rejected.

4. If we check the assumption of annual maxima coming from GPD-Poisson distribution, analogous results are obtained. p-values from Cramer-von Mises test associated with GEV annual maxima fitting are mostly above significance level $\alpha = 0.05$, i.e. the hypothesis of annual maxima coming from GPD-Poisson or GEV distribution is rarely rejected.
5. In the spatial model, both optimal parameters γ_0 and γ_1 from the shape parameterization (10) are equal to zero, i.e. all fitted distributions correspond to Gumbel.
6. Hypothesis tests related to spatial fitting provide the same diagnostics than the local model. The main assumptions required for extreme characterization through GPD-Poisson distribution are rarely rejected, which also confirms good fitting diagnostics.
7. All results associated with the rest of timescales: 20, 30, 60, 120, 180, 240, 360, 720 and 1440 minutes are analogous.

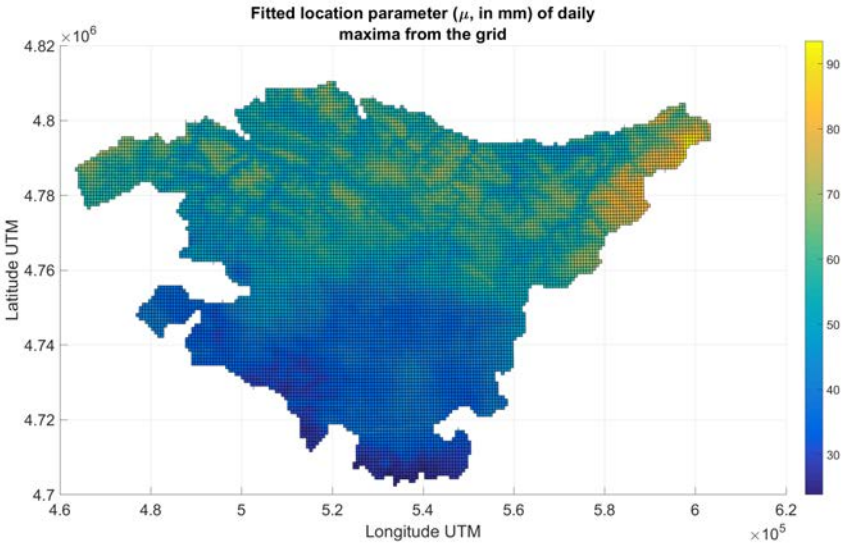

(a) Gumbel location parameter μ in mm.

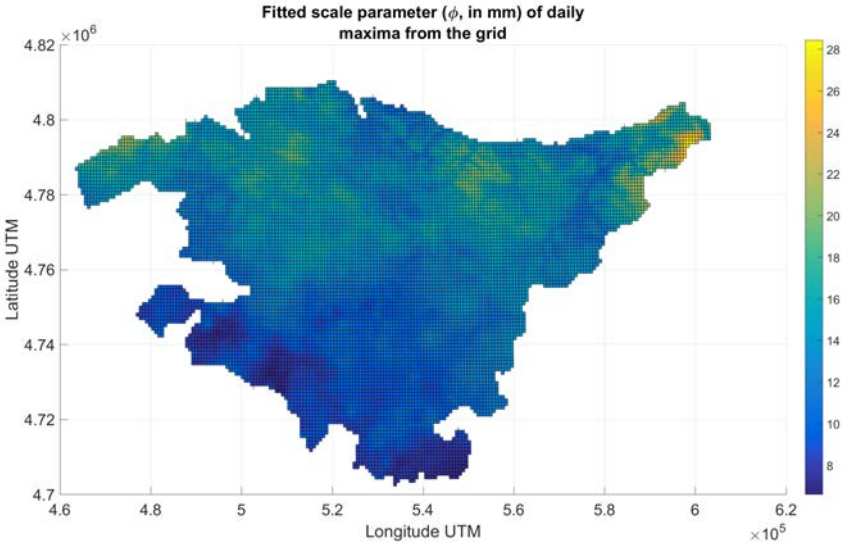

(b) Gumbel scale parameter σ in mm.

Fig. 3 Gumbel fitted parameters associated with daily annual maxima rainfall over the 1 km spatial resolution grid.

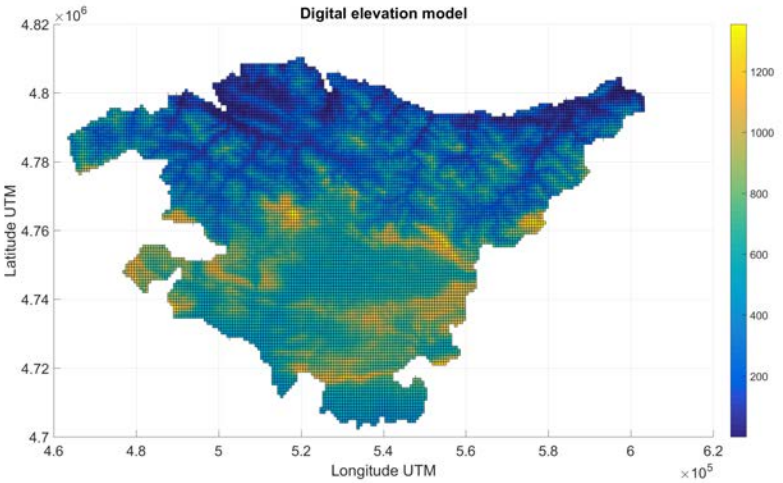

Fig. 4 Digital elevation model in meters over the study area.

Table 1: Local (L) and spatial (S) EV fitting related to 10 minutes timescale at available rain gauges.

Name	**Type**	λ(e/year)	σ(mm)	ξ	u(mm)	μ(mm)	ψ(mm)	p_{W}	p_1	p_2	p_3	p_4	$p_{\mathrm{W}}^{\mathrm{max}}$
Ilarduia	L	2.283	2.900	0.000	4.600	6.994	2.900	0.597	0.123	0.260	0.358	0.453	0.686
Ilarduia	S	2.291	2.855	0.000	4.600	6.967	2.855	0.599	0.123	0.260	0.359	0.453	0.684
Berriatua	L	2.479	2.138	**0.258**	4.700	6.886	2.701	0.256	0.126	0.245	0.418	**0.041**	0.132
Berriatua	S	2.426	2.855	0.000	4.700	7.230	2.855	0.215	0.051	0.140	0.268	0.054	**0.010**
Iruzubieta	L	1.712	2.088	0.000	4.772	5.895	2.088	0.375	0.902	0.935	0.524	0.141	0.886
Iruzubieta	S	2.480	2.855	0.000	4.772	7.366	2.855	0.326	0.913	0.938	0.528	0.145	0.882
Beluntza	L	2.069	3.133	0.000	3.667	5.944	3.133	0.488	0.196	0.224	0.380	0.543	**0.033**
Beluntza	S	3.574	2.860	0.000	3.667	7.310	2.860	0.487	0.197	0.227	0.382	0.546	**0.034**
Sarria	L	2.433	3.395	0.000	4.418	7.437	3.395	0.310	0.882	0.498	0.669	0.632	0.251
Sarria	S	2.661	2.857	0.000	4.418	7.215	2.857	0.316	0.883	0.497	0.669	0.630	0.276
Subijana (Peaje)	L	2.575	2.798	0.000	4.271	6.918	2.798	0.561	0.836	0.716	0.726	0.690	0.880
Subijana (Peaje)	S	2.429	2.850	0.000	4.271	6.800	2.850	0.561	0.837	0.717	0.726	0.691	0.877
Behobia	L	2.687	2.623	0.000	5.102	7.694	2.623	0.223	0.570	0.615	0.804	0.855	0.088
Behobia	S	2.580	2.862	0.000	5.102	7.814	2.862	0.231	0.571	0.615	0.804	0.857	0.085
Endara	L	1.716	3.090	0.000	7.462	9.131	3.090	0.516	0.484	0.704	0.381	0.546	0.881
Endara	S	1.309	2.870	0.000	7.462	8.235	2.870	0.510	0.483	0.702	0.381	0.545	0.880
Endara	L	2.891	2.767	0.000	6.200	9.138	2.767	0.225	0.438	0.273	0.445	0.606	0.910
Endara	S	2.032	2.870	0.000	6.200	8.235	2.870	0.230	0.437	0.273	0.446	0.607	0.904
Endara antigua	L	2.583	4.512	0.000	6.300	10.582	4.512	0.799	0.824	0.944	0.982	0.200	0.419
Endara antigua	S	1.876	2.868	0.000	6.300	8.104	2.868	0.766	0.820	0.940	0.980	0.196	0.413
Mungia (DAEM)	L	2.520	2.603	0.000	4.900	7.306	2.603	0.280	0.751	0.726	0.878	0.368	0.498
Mungia (DAEM)	S	2.205	2.859	0.000	4.900	7.161	2.859	0.294	0.743	0.725	0.877	0.368	0.548
Aixola	L	2.882	2.426	**0.273**	4.300	7.277	3.238	0.181	0.518	0.795	0.318	0.202	0.715
Aixola	S	3.086	2.858	0.000	4.300	7.521	2.858	0.159	0.437	0.669	0.402	0.240	0.235
Altzola	L	2.938	1.944	0.000	4.500	6.595	1.944	0.517	0.394	0.656	0.815	0.886	0.077
Altzola	S	2.732	2.861	0.000	4.500	7.375	2.861	0.599	0.383	0.635	0.798	0.872	0.082
Arantzazu Pluviometro	L	2.248	2.515	0.000	5.200	7.237	2.515	0.058	0.356	0.255	0.434	0.291	0.482
Arantzazu Pluviometro	S	2.046	2.856	0.000	5.200	7.245	2.856	0.060	0.354	0.255	0.434	0.288	0.526
Araotz	L	2.582	3.155	0.000	4.900	7.893	3.155	0.689	0.678	0.086	0.174	0.284	0.168
Araotz	S	2.194	2.856	0.000	4.900	7.144	2.856	0.673	0.675	0.087	0.176	0.287	0.181
Arrasate	L	2.456	3.161	0.000	4.100	6.940	3.161	0.152	0.698	0.910	0.969	0.913	**0.043**
Arrasate	S	3.036	2.862	0.000	4.100	7.278	2.862	0.145	0.697	0.910	0.968	0.913	0.058

Continue

Name	**Type**	λ(e/year)	σ(mm)	ξ	u(mm)	μ(mm)	ψ(mm)	p_{W}	p_1	p_2	p_3	p_4	$p_{\mathrm{W}}^{\mathrm{max}}$
Eitzaga	L	2.800	2.117	0.000	3.700	5.880	2.117	0.358	0.623	0.454	0.652	0.801	0.453
Eitzaga	S	3.804	2.858	0.000	3.700	7.519	2.858	0.320	0.644	0.448	0.645	0.794	0.426
Elosua	L	2.320	3.279	0.000	4.600	7.359	3.279	0.686	0.169	0.314	0.446	0.561	0.888
Elosua	S	2.855	2.862	0.000	4.600	7.602	2.862	0.675	0.171	0.316	0.448	0.564	0.947
Lastur Pluviometro	L	2.478	1.941	**0.254**	5.000	6.981	2.444	0.262	0.479	0.444	0.633	0.734	0.756
Lastur Pluviometro	S	2.440	2.864	0.000	5.000	7.555	2.864	0.223	0.281	0.346	0.536	0.687	0.094
Mendaro	L	2.456	2.584	0.000	4.800	7.122	2.584	**0.046**	0.157	0.191	0.227	0.284	**0.018**
Mendaro	S	2.475	2.861	0.000	4.800	7.393	2.861	**0.048**	0.157	0.191	0.227	0.284	**0.014**
Oñati	L	2.712	2.657	0.000	4.316	6.966	2.657	0.219	0.590	0.376	0.572	0.605	0.223
Oñati	S	2.805	2.857	0.000	4.316	7.262	2.857	0.225	0.589	0.378	0.574	0.608	0.205
San Prudentzio	L	2.626	3.371	0.000	4.300	7.555	3.371	0.309	0.807	0.918	0.957	0.595	0.180
San Prudentzio	S	2.749	2.858	0.000	4.300	7.190	2.858	0.277	0.810	0.916	0.958	0.599	0.225
Urkulu	L	2.515	2.857	0.000	4.800	7.435	2.857	0.217	0.664	0.886	0.892	0.928	0.797
Urkulu	S	2.254	2.855	0.000	4.800	7.121	2.855	0.217	0.664	0.886	0.892	0.928	0.799
Moreda	L	2.550	2.645	0.000	4.250	6.726	2.645	0.549	0.727	0.680	0.834	0.906	0.794
Moreda	S	2.284	2.846	0.000	4.250	6.600	2.846	0.549	0.726	0.678	0.832	0.905	0.807
Paganos	L	2.813	2.964	0.000	3.629	6.695	2.964	0.494	0.353	0.637	0.273	0.332	0.159
Paganos	S	2.902	2.849	0.000	3.629	6.665	2.849	0.482	0.353	0.637	0.273	0.333	0.163
Iturrieta (Granja)	L	2.103	3.278	0.000	5.000	7.436	3.278	0.232	0.912	0.848	0.421	0.569	0.100
Iturrieta (Granja)	S	1.983	2.855	0.000	5.000	6.955	2.855	0.215	0.907	0.847	0.424	0.572	0.117
Kanpezu	L	2.750	3.720	0.000	4.300	8.063	3.720	0.142	0.980	0.994	0.941	0.853	0.053
Kanpezu	S	2.487	2.855	0.000	4.300	6.901	2.855	0.130	0.984	0.993	0.945	0.859	0.064
Navarrete	L	2.901	2.441	0.000	4.775	7.375	2.441	0.702	0.723	0.541	0.740	0.803	0.819
Navarrete	S	2.084	2.850	0.000	4.775	6.869	2.850	0.745	0.725	0.538	0.736	0.801	0.749
Roitegi	L	2.927	1.894	0.000	3.456	5.490	1.894	0.149	0.971	0.927	0.545	0.625	0.382
Roitegi	S	3.313	2.855	0.000	3.456	6.876	2.855	0.165	0.958	0.926	0.552	0.626	0.434
Abusu	L	2.723	2.689	0.000	4.900	7.594	2.689	0.650	0.316	0.600	0.690	0.829	**0.012**
Abusu	S	2.242	2.861	0.000	4.900	7.210	2.861	0.665	0.319	0.603	0.693	0.831	**0.008**
Altube (Peaje)	L	2.172	3.887	0.000	4.300	7.316	3.887	0.502	0.128	0.211	0.270	0.117	0.926
Altube (Peaje)	S	2.723	2.859	0.000	4.300	7.164	2.859	0.421	0.126	0.213	0.273	0.122	0.904
Amorebieta	L	2.695	2.572	0.000	4.500	7.050	2.572	0.354	0.947	0.918	0.681	0.380	0.336
Amorebieta	S	2.585	2.857	0.000	4.500	7.213	2.857	0.370	0.942	0.918	0.681	0.383	0.299
Aranguren	L	2.337	2.533	0.000	4.000	6.150	2.533	0.654	0.612	0.370	0.299	0.426	0.307
Aranguren	S	2.936	2.856	0.000	4.000	7.075	2.856	0.678	0.615	0.366	0.298	0.424	0.293
Arboleda	L	2.823	1.428	0.000	4.200	5.682	1.428	**0.008**	0.990	0.725	**0.049**	0.087	0.744

Continue

Name	**Type**	λ(e/year)	σ(mm)	ξ	u(mm)	μ(mm)	ψ(mm)	p_{W}	p_1	p_2	p_3	p_4	$p_{\mathrm{W}}^{\mathrm{max}}$
Arboleda	S	3.193	2.861	0.000	4.200	7.521	2.861	**0.015**	0.975	0.757	0.054	0.095	0.665
Areta	L	2.715	3.390	0.000	4.400	7.787	3.390	0.742	0.974	0.733	0.761	0.882	0.192
Areta	S	2.651	2.859	0.000	4.400	7.187	2.859	0.711	0.964	0.724	0.753	0.877	0.227
Balmaseda	L	2.421	2.500	0.000	4.282	6.493	2.500	0.744	0.344	0.623	0.783	0.733	0.979
Balmaseda	S	2.682	2.857	0.000	4.282	7.100	2.857	0.733	0.340	0.615	0.776	0.728	0.977
Berna	L	2.847	2.155	0.000	4.400	6.655	2.155	**0.027**	0.411	0.197	0.355	0.285	**0.035**
Berna	S	2.686	2.857	0.000	4.400	7.222	2.857	**0.041**	0.402	0.196	0.353	0.290	**0.019**
Derio	L	2.740	2.115	0.000	4.700	6.832	2.115	0.177	0.305	0.580	0.778	0.879	0.987
Derio	S	2.454	2.863	0.000	4.700	7.270	2.863	0.176	0.300	0.571	0.771	0.875	0.983
Deusto	L	2.690	2.741	0.000	4.100	6.812	2.741	0.254	0.163	0.318	0.408	0.471	0.427
Deusto	S	2.941	2.859	0.000	4.100	7.185	2.859	0.263	0.164	0.319	0.409	0.471	0.425
Elorrio	L	2.543	2.457	0.000	4.000	6.293	2.457	0.072	0.117	0.252	0.155	0.217	0.207
Elorrio	S	3.047	2.853	0.000	4.000	7.179	2.853	0.082	0.116	0.249	0.153	0.215	0.189
Galindo (CABB)	L	2.588	1.618	0.000	3.788	5.326	1.618	0.443	0.155	0.363	0.226	0.240	**0.018**
Galindo (CABB)	S	3.318	2.859	0.000	3.788	7.217	2.859	0.370	0.166	0.382	0.234	0.245	**0.014**
Gardea	L	2.476	2.825	0.000	4.700	7.261	2.825	0.395	0.493	0.191	0.345	0.442	0.252
Gardea	S	2.372	2.858	0.000	4.700	7.169	2.858	0.395	0.492	0.190	0.345	0.442	0.241
Igorre	L	2.555	2.562	0.000	4.700	7.103	2.562	0.745	0.466	0.511	0.350	0.490	0.453
Igorre	S	2.441	2.860	0.000	4.700	7.252	2.860	0.749	0.462	0.509	0.345	0.483	0.394
Iurreta	L	2.857	1.567	0.000	4.049	5.694	1.567	0.471	0.535	0.823	0.940	0.619	0.169
Iurreta	S	3.035	2.855	0.000	4.049	7.219	2.855	0.569	0.472	0.770	0.911	0.600	0.170
La Garbea	L	2.350	1.815	**0.339**	3.500	5.298	2.425	0.063	0.935	0.952	0.378	0.537	0.514
La Garbea	S	4.028	2.859	0.000	3.500	7.483	2.859	0.071	0.761	0.950	0.423	0.585	0.068
Llodio	L	2.551	2.789	0.000	3.600	6.212	2.789	0.853	0.188	0.094	0.193	0.098	0.468
Llodio	S	3.562	2.859	0.000	3.600	7.232	2.859	0.855	0.188	0.094	0.192	0.097	0.498
Mañaria	L	2.738	1.432	**0.547**	4.299	6.224	2.485	0.223	0.480	0.748	0.640	0.793	0.604
Mañaria	S	2.911	2.857	0.000	4.299	7.352	2.857	0.278	0.246	0.501	0.665	0.806	0.435
Ordunte	L	2.358	3.002	0.000	4.000	6.575	3.002	0.669	0.070	0.163	0.293	0.442	0.136
Ordunte	S	3.291	2.860	0.000	4.000	7.406	2.860	0.671	0.070	0.164	0.294	0.443	0.166
Orduña	L	2.280	2.469	0.000	4.000	6.035	2.469	0.742	0.721	0.923	0.695	0.306	0.911
Orduña	S	2.825	2.853	0.000	4.000	6.963	2.853	0.735	0.723	0.924	0.698	0.301	0.897
Orozko (Altube)	L	2.496	1.609	**0.378**	4.500	6.259	2.274	**0.045**	0.500	0.729	0.816	0.572	0.352
Orozko (Altube)	S	2.568	2.858	0.000	4.500	7.196	2.858	**0.026**	0.643	0.799	0.844	0.538	0.089
Punta Galea (DAEM)	L	2.455	3.221	0.000	4.700	7.593	3.221	0.740	0.085	0.157	0.200	0.203	0.092
Punta Galea (DAEM)	S	2.501	2.859	0.000	4.700	7.320	2.859	0.740	0.083	0.154	0.196	0.197	0.118

Continue

Name	**Type**	λ(e/year)	σ(mm)	ξ	u(mm)	μ(mm)	ψ(mm)	p_{W}	p_1	p_2	p_3	p_4	$p_{\mathrm{W}}^{\mathrm{max}}$
Sangroniz	L	2.980	1.992	0.000	4.100	6.275	1.992	**0.032**	0.058	0.139	0.159	0.269	0.204
Sangroniz	S	3.006	2.860	0.000	4.100	7.248	2.860	**0.041**	0.060	0.141	0.161	0.271	0.182
Saratxo	L	2.316	2.177	0.000	4.600	6.428	2.177	0.152	0.946	0.868	0.952	0.986	0.688
Saratxo	S	2.383	2.857	0.000	4.600	7.081	2.857	0.191	0.914	0.850	0.943	0.982	0.619
Sodupe-Herrerias	L	2.890	2.498	0.000	4.200	6.850	2.498	0.172	0.468	0.621	0.448	0.382	0.738
Sodupe-Herrerias	S	2.823	2.857	0.000	4.200	7.165	2.857	0.189	0.476	0.623	0.449	0.383	0.728
Sodupe-Kadagua	L	2.927	2.070	0.000	2.597	4.820	2.070	0.571	0.778	0.239	0.386	0.241	0.302
Sodupe-Kadagua	S	4.699	2.856	0.000	2.597	7.017	2.856	0.516	0.765	0.247	0.395	0.249	0.323
Urkizu	L	2.424	2.905	0.000	4.300	6.872	2.905	0.592	0.249	0.399	0.594	0.523	0.548
Urkizu	S	2.809	2.859	0.000	4.300	7.253	2.859	0.590	0.249	0.399	0.595	0.524	0.587
Zaratamo	L	2.307	3.126	0.000	4.111	6.724	3.126	**0.023**	0.837	0.978	0.450	0.586	0.276
Zaratamo	S	2.976	2.861	0.000	4.111	7.231	2.861	**0.021**	0.832	0.977	0.453	0.588	0.304
Herrera (Puerto)	L	2.795	3.099	0.000	4.300	7.485	3.099	0.109	0.766	0.931	0.880	0.699	0.788
Herrera (Puerto)	S	2.455	2.850	0.000	4.300	6.860	2.850	0.104	0.767	0.932	0.880	0.702	0.775
Laurgain	L	2.143	3.110	0.000	6.000	8.371	3.110	0.328	0.683	0.550	0.436	0.435	**0.018**
Laurgain	S	1.468	2.856	0.000	6.000	7.096	2.856	0.313	0.678	0.551	0.436	0.433	**0.016**
Cerroja (balsa)	L	2.955	2.239	0.000	3.700	6.126	2.239	0.071	0.405	0.581	0.771	0.682	0.512
Cerroja (balsa)	S	3.937	2.860	0.000	3.700	7.620	2.860	0.074	0.407	0.584	0.774	0.684	0.548
Oiz	L	2.543	1.691	**0.255**	3.100	4.881	2.144	0.166	**0.002**	**0.007**	**0.012**	**0.009**	0.082
Oiz	S	5.012	2.859	0.000	3.100	7.709	2.859	0.161	**0.003**	**0.011**	**0.020**	**0.017**	**0.004**
Oleta	L	2.431	2.783	0.000	4.700	7.171	2.783	0.487	0.987	0.825	0.943	0.968	0.487
Oleta	S	2.396	2.853	0.000	4.700	7.194	2.853	0.490	0.986	0.825	0.943	0.968	0.480
Jaizkibel	L	2.463	1.800	0.000	4.900	6.523	1.800	0.785	0.143	0.240	0.414	0.574	0.326
Jaizkibel	S	3.115	2.869	0.000	4.900	8.160	2.869	0.820	0.143	0.237	0.411	0.571	0.326
Oiartzun	L	2.588	2.160	0.000	5.700	7.754	2.160	0.099	0.690	0.734	0.562	0.715	**0.028**
Oiartzun	S	1.887	2.858	0.000	5.700	7.515	2.858	0.087	0.704	0.750	0.558	0.713	**0.014**
Oiartzun DFG	L	2.546	2.880	0.000	6.200	8.892	2.880	0.548	0.730	0.406	0.566	0.214	0.494
Oiartzun DFG	S	1.933	2.867	0.000	6.200	8.089	2.867	0.546	0.730	0.407	0.567	0.214	0.454
Almike (Bermeo)	L	2.757	2.727	0.000	4.400	7.165	2.727	**0.007**	0.777	0.568	0.768	0.591	0.517
Almike (Bermeo)	S	2.754	2.856	0.000	4.400	7.294	2.856	**0.007**	0.776	0.566	0.767	0.589	0.506
Arteaga	L	2.656	2.900	0.000	4.100	6.932	2.900	0.710	**0.019**	**0.022**	**0.050**	**0.041**	0.169
Arteaga	S	2.965	2.854	0.000	4.100	7.201	2.854	0.711	**0.019**	**0.022**	**0.050**	**0.041**	0.168
Matxitxako	L	2.548	2.487	0.000	5.000	7.326	2.487	0.324	0.172	0.354	0.557	0.715	0.660
Matxitxako	S	2.665	2.861	0.000	5.000	7.805	2.861	0.335	0.173	0.358	0.560	0.719	0.636

Continue

Name	**Type**	λ(e/year)	σ(mm)	ξ	u(mm)	μ(mm)	ψ(mm)	p_{W}	p_1	p_2	p_3	p_4	$p_{\mathrm{W}}^{\mathrm{max}}$
Muxika	L	2.570	2.092	**0.267**	4.501	6.747	2.692	0.279	0.304	0.236	0.389	0.506	0.059
Muxika	S	2.518	2.855	0.000	4.501	7.138	2.855	0.267	0.206	0.178	0.318	0.424	**0.002**
Espejo	L	2.763	4.121	0.000	4.100	8.289	4.121	0.170	0.876	0.894	0.907	0.641	0.649
Espejo	S	2.494	2.849	0.000	4.100	6.703	2.849	0.179	0.861	0.891	0.904	0.644	0.684
Agauntza	L	2.300	3.258	0.000	5.300	8.013	3.258	0.170	0.856	0.195	0.200	0.228	0.328
Agauntza	S	1.977	2.855	0.000	5.300	7.247	2.855	0.156	0.869	0.199	0.201	0.230	0.355
Alegia	L	1.617	3.388	0.000	6.666	8.294	3.388	0.241	0.871	0.484	0.222	0.202	0.805
Alegia	S	1.245	2.854	0.000	6.666	7.292	2.854	0.254	0.875	0.485	0.218	0.200	0.831
Ameraun	L	1.945	2.688	0.000	6.300	8.088	2.688	0.101	0.444	0.709	0.654	0.742	**0.035**
Ameraun	S	1.731	2.861	0.000	6.300	7.869	2.861	0.101	0.446	0.712	0.658	0.744	**0.027**
Amundarain	L	2.804	3.179	0.000	4.700	7.978	3.179	0.688	0.755	0.588	0.397	0.537	0.898
Amundarain	S	2.439	2.855	0.000	4.700	7.245	2.855	0.669	0.754	0.596	0.401	0.540	0.900
Araxes	L	2.606	2.677	0.000	4.547	7.111	2.677	0.137	0.280	0.518	0.566	0.722	0.804
Araxes	S	2.752	2.854	0.000	4.547	7.436	2.854	0.136	0.280	0.517	0.566	0.721	0.808
Arriaran DFG	L	2.366	2.507	0.000	5.000	7.159	2.507	0.114	**0.042**	**0.030**	**0.014**	**0.031**	0.738
Arriaran DFG	S	2.300	2.860	0.000	5.000	7.382	2.860	0.119	**0.041**	**0.030**	**0.014**	**0.031**	0.733
Belauntza	L	2.844	2.939	0.000	4.800	7.872	2.939	**0.021**	0.726	0.918	0.800	0.906	0.432
Belauntza	S	2.643	2.855	0.000	4.800	7.575	2.855	**0.020**	0.727	0.919	0.802	0.908	0.434
Berastegi	L	2.746	2.822	0.000	5.300	8.151	2.822	0.615	0.538	0.467	0.213	0.121	0.841
Berastegi	S	2.490	2.860	0.000	5.300	7.909	2.860	0.615	0.538	0.467	0.213	0.121	0.834
Bidania	L	1.808	3.155	**-0.364**	5.300	6.981	2.543	0.758	0.640	0.499	0.666	0.712	0.446
Bidania	S	2.268	2.859	0.000	5.300	7.642	2.859	0.801	0.555	0.468	0.624	0.688	0.546
Estanda	L	2.585	3.704	**-0.310**	4.800	7.848	2.760	0.822	0.983	0.662	0.821	0.717	0.794
Estanda	S	2.259	2.857	0.000	4.800	7.128	2.857	**0.000**	0.937	0.569	0.770	0.763	0.947
Ibiur (Estación)	L	1.553	3.515	0.000	5.526	7.073	3.515	0.259	0.917	0.475	0.497	0.658	0.092
Ibiur (Estación)	S	1.898	2.856	0.000	5.526	7.356	2.856	0.234	0.920	0.480	0.501	0.663	0.121
Ibiur Pluviometro	L	2.894	2.601	0.000	5.000	7.764	2.601	0.086	0.141	0.059	0.104	0.172	0.389
Ibiur Pluviometro	S	2.177	2.855	0.000	5.000	7.221	2.855	0.093	0.142	0.059	0.104	0.173	0.342
Lareo	L	2.676	2.437	0.000	5.000	7.399	2.437	0.175	0.109	0.272	0.285	0.084	0.944
Lareo	S	2.451	2.858	0.000	5.000	7.562	2.858	0.159	0.107	0.268	0.279	0.082	0.903
Lasarte	L	2.826	2.438	0.000	5.209	7.741	2.438	0.478	0.761	0.944	0.495	0.570	0.274
Lasarte	S	2.157	2.855	0.000	5.209	7.403	2.855	0.468	0.760	0.944	0.494	0.568	0.315
Leitzaran (Andoain)	L	2.735	2.839	0.000	4.800	7.657	2.839	0.626	0.798	0.628	0.137	0.234	**0.040**
Leitzaran (Andoain)	S	2.416	2.854	0.000	4.800	7.317	2.854	0.628	0.798	0.628	0.137	0.234	**0.037**
Ordizia	L	2.662	2.539	0.000	4.900	7.386	2.539	0.585	0.547	0.746	0.581	0.531	0.504

Continue

Name	**Type**	λ(e/year)	σ(mm)	ξ	u(mm)	μ(mm)	ψ(mm)	p_{W}	p_1	p_2	p_3	p_4	$p_{\mathrm{W}}^{\mathrm{max}}$
Ordizia	S	2.319	2.857	0.000	4.900	7.303	2.857	0.548	0.550	0.755	0.585	0.533	0.525
Troya	L	2.901	2.635	0.000	4.400	7.207	2.635	0.130	0.241	0.401	0.464	0.417	0.814
Troya	S	2.712	2.858	0.000	4.400	7.252	2.858	0.128	0.240	0.400	0.464	0.417	0.811
Zaldibia	L	2.634	2.910	0.000	5.200	8.019	2.910	0.234	0.877	0.182	0.332	0.411	**0.046**
Zaldibia	S	2.225	2.857	0.000	5.200	7.486	2.857	0.232	0.877	0.182	0.332	0.411	**0.043**
Zarautz (DAEM)	L	2.495	2.815	0.000	5.100	7.674	2.815	0.799	0.194	0.217	0.177	0.220	0.083
Zarautz (DAEM)	S	2.069	2.856	0.000	5.100	7.176	2.856	0.802	0.194	0.217	0.177	0.221	0.071
Zegama	L	2.627	3.264	0.000	5.000	8.153	3.264	0.100	0.481	0.082	0.134	0.202	0.227
Zegama	S	2.146	2.857	0.000	5.000	7.181	2.857	0.090	0.480	0.079	0.132	0.198	0.233
Zizurkil	L	2.572	2.392	0.000	4.500	6.760	2.392	0.719	0.289	0.426	0.509	0.585	0.839
Zizurkil	S	2.576	2.854	0.000	4.500	7.201	2.854	0.702	0.287	0.427	0.513	0.590	0.867
Aitzu	L	2.946	2.318	0.000	4.269	6.773	2.318	0.059	0.364	0.609	0.748	0.866	0.093
Aitzu	S	2.950	2.861	0.000	4.269	7.364	2.861	0.071	0.366	0.617	0.752	0.869	0.072
Aizarnazabal	L	2.619	2.118	0.000	4.900	6.939	2.118	0.141	0.806	0.894	0.966	0.981	0.497
Aizarnazabal	S	2.105	2.857	0.000	4.900	7.027	2.857	0.176	0.819	0.904	0.969	0.982	0.406
Barrendiola DFG meteo	L	2.516	2.534	0.000	5.136	7.474	2.534	0.065	0.975	0.401	0.285	0.364	0.858
Barrendiola DFG meteo	S	2.235	2.858	0.000	5.136	7.435	2.858	0.069	0.970	0.401	0.287	0.366	0.853
Erdoizta	L	2.153	3.034	0.000	5.400	7.727	3.034	0.871	0.869	0.986	0.616	0.666	0.728
Erdoizta	S	2.024	2.860	0.000	5.400	7.417	2.860	0.868	0.870	0.986	0.617	0.665	0.731
Ibaieder	L	1.719	2.426	0.000	5.914	7.229	2.426	0.113	0.704	0.233	**0.035**	0.072	**0.042**
Ibaieder	S	1.495	2.857	0.000	5.914	7.063	2.857	0.130	0.701	0.233	**0.035**	0.071	**0.031**
Matxinbenta	L	2.835	2.562	0.000	4.300	6.970	2.562	0.512	0.945	0.083	0.152	0.220	0.791
Matxinbenta	S	2.903	2.858	0.000	4.300	7.346	2.858	0.529	0.941	0.083	0.153	0.221	0.816
BARRENDIOLA	L	2.981	2.483	0.000	4.200	6.912	2.483	0.839	0.090	0.134	0.252	0.325	0.991
BARRENDIOLA	S	3.084	2.857	0.000	4.200	7.417	2.857	0.859	0.090	0.133	0.251	0.325	0.990
Añarbe (estación)	L	2.058	2.731	0.000	6.285	8.257	2.731	0.411	0.943	0.966	0.981	0.611	0.059
Añarbe (estación)	S	1.751	2.863	0.000	6.285	7.888	2.863	0.419	0.946	0.967	0.981	0.610	**0.047**
Artikutza Eskas	L	1.871	3.168	0.000	7.196	9.180	3.168	0.261	0.803	0.099	0.201	0.321	0.259
Artikutza Eskas	S	1.504	2.868	0.000	7.196	8.366	2.868	0.257	0.812	0.100	0.203	0.325	0.264
Ereñozu	L	2.945	2.114	**0.287**	5.891	8.568	2.884	0.839	0.237	0.464	0.314	0.272	0.561
Ereñozu	S	1.744	2.857	0.000	5.891	7.480	2.857	0.804	0.206	0.414	0.231	0.213	0.076
Igeldo DFG	L	2.749	2.536	0.000	6.000	8.564	2.536	0.246	0.478	0.760	0.720	0.855	0.469
Igeldo DFG	S	1.587	2.858	0.000	6.000	7.321	2.858	0.259	0.484	0.765	0.725	0.858	0.316
Miramon	L	1.806	1.942	0.000	5.800	6.948	1.942	0.487	0.495	0.282	0.467	0.557	0.791
Miramon	S	1.688	2.858	0.000	5.800	7.296	2.858	0.468	0.482	0.272	0.454	0.548	0.805

Continue

Name	**Type**	λ(e/year)	σ(mm)	ξ	u(mm)	μ(mm)	ψ(mm)	p_{W}	p_1	p_2	p_3	p_4	$p_{\mathrm{W}}^{\mathrm{max}}$
Añarbe (estación)	L	2.027	2.781	0.000	6.300	8.265	2.781	0.335	0.713	0.894	0.902	0.691	0.056
Añarbe (estación)	S	1.742	2.863	0.000	6.300	7.888	2.863	0.341	0.710	0.892	0.901	0.690	**0.047**
Abetxuko (DAEM)	L	2.727	2.630	0.000	3.400	6.038	2.630	0.738	0.295	0.567	0.765	0.715	0.776
Abetxuko (DAEM)	S	3.293	2.851	0.000	3.400	6.797	2.851	0.758	0.296	0.569	0.767	0.716	0.786
Alegria (canal)	L	2.934	2.762	0.000	3.600	6.572	2.762	0.086	0.132	0.265	0.216	0.329	0.087
Alegria (canal)	S	3.039	2.852	0.000	3.600	6.771	2.852	0.089	0.132	0.265	0.216	0.330	0.083
Arkaute I	L	2.548	2.795	0.000	4.300	6.914	2.795	0.287	0.761	0.834	0.587	0.731	0.400
Arkaute I	S	2.419	2.853	0.000	4.300	6.820	2.853	0.288	0.760	0.836	0.587	0.731	0.383
Barazar	L	2.731	2.427	0.000	4.500	6.938	2.427	0.418	0.515	0.357	0.560	0.647	0.366
Barazar	S	2.684	2.860	0.000	4.500	7.324	2.860	0.440	0.524	0.363	0.567	0.651	0.330
Etura	L	2.629	2.178	0.000	3.400	5.506	2.178	0.187	0.926	0.398	0.584	0.529	0.088
Etura	S	3.296	2.852	0.000	3.400	6.802	2.852	0.173	0.931	0.398	0.579	0.518	0.074
Gasteiz (Lakua)	L	2.793	2.973	0.000	3.700	6.754	2.973	0.574	0.806	0.238	0.349	0.394	0.969
Gasteiz (Lakua)	S	2.986	2.852	0.000	3.700	6.820	2.852	0.561	0.808	0.237	0.348	0.393	0.973
Gorbea (Embalse)	L	2.372	2.917	0.000	4.000	6.520	2.917	0.094	0.066	0.166	0.308	0.461	0.191
Gorbea (Embalse)	S	3.196	2.858	0.000	4.000	7.321	2.858	0.093	0.066	0.167	0.308	0.461	0.207
Kapildui	L	2.763	3.272	0.000	3.700	7.026	3.272	0.428	0.322	0.228	0.358	0.385	0.225
Kapildui	S	3.147	2.851	0.000	3.700	6.969	2.851	0.407	0.318	0.227	0.357	0.386	0.241
Otxandio (Iberdrola)	L	2.818	3.231	0.000	4.656	8.003	3.231	0.365	0.725	0.312	0.375	0.501	0.269
Otxandio (Iberdrola)	S	2.537	2.857	0.000	4.656	7.315	2.857	0.373	0.731	0.307	0.368	0.494	0.297
Ozaeta (Iberdrola)	L	2.754	3.972	0.000	4.300	8.323	3.972	0.421	0.190	**0.025**	0.054	0.104	0.300
Ozaeta (Iberdrola)	S	2.495	2.855	0.000	4.300	6.910	2.855	0.360	0.180	**0.023**	0.051	0.099	0.500
Salvatierra	L	2.542	3.060	0.000	4.300	7.154	3.060	0.341	0.587	0.511	0.628	0.682	0.613
Salvatierra	S	2.482	2.855	0.000	4.300	6.896	2.855	0.325	0.588	0.511	0.630	0.684	0.626
Trebiño	L	2.477	2.195	0.000	3.833	5.824	2.195	0.619	0.373	0.463	0.633	0.735	0.179
Trebiño	S	2.740	2.851	0.000	3.833	6.706	2.851	0.592	0.357	0.454	0.623	0.722	0.195
Urkiola	L	2.684	4.139	0.000	4.454	8.541	4.139	0.176	0.931	0.969	0.393	0.504	**0.038**
Urkiola	S	2.850	2.859	0.000	4.454	7.448	2.859	0.126	0.947	0.970	0.390	0.499	0.078
Zaldiaran (Repetidor)	L	2.941	3.127	0.000	3.500	6.873	3.127	**0.026**	0.327	0.614	0.800	0.896	0.912
Zaldiaran (Repetidor)	S	3.274	2.852	0.000	3.500	6.883	2.852	**0.024**	0.329	0.617	0.801	0.897	0.915
Zambrana	L	2.857	2.433	0.000	3.900	6.454	2.433	0.338	0.482	0.330	0.148	0.225	0.482
Zambrana	S	2.569	2.848	0.000	3.900	6.588	2.848	0.367	0.480	0.334	0.150	0.227	0.406

Apparently, both local and spatial fittings at locations where rain gauges exist seem to be appropriate. However, we need to define an objective criteria to decide which one is more consistent, and more important, does the spatial model hold the desired characteristics set out previously (see Section 1)? Let us analyse results with respect to those features:

1. **Being robust with respect to abnormally high records (outliers).** In this particular case, there are several locations where one single extreme event pushes the tail towards Frechet. For example, Figure 5 shows a return period fitting diagnostic plot for precipitation duration of 1440 minutes at Lastur (LAST) rain gauge. Local fitting corresponds to Frechet type with a positive shape parameter, while the spatial fitting corresponds to Gumbel, which is more consistent with respect to Gumbel fittings around this location. In both cases, the hypothesis of annual maxima coming from the fitted distribution can not be rejected with p-values equal to 0.87 and 0.41, respectively. However, the maximum record of 207.2 mm has less than 100 years of return period for the local fitting, while for the spatial case it corresponds to a return period of about 167 years. Note that the probability

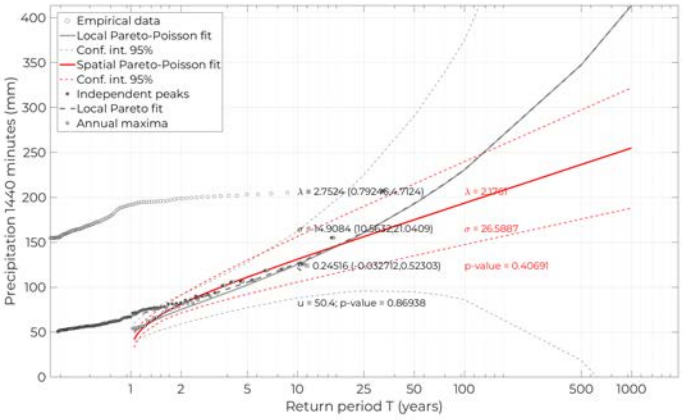

Fig. 5 Fitted return periods for 1440 minutes timescale at Lastur (LAST) rain gauge.

of occurrence of a 167-year return period ($\lambda = 1/167$) over a record of 31 years corresponds to:

$$1 - \text{Prob}(Y = 0)^{31} = 1 - \left(\frac{\lambda^0}{0!}e^{-\lambda}\right)^{31} = 0.17 \tag{19}$$

which is likely. This result and the Gumbel fits associated to close locations shows the coherence of spatial fitted model at this specific rain gauge.

2. **Being robust in case the data provided by a rain gauge contains systematic biases due to location, exposure to wind, obstacles,**

or other causes. In this particular case, we know from a previous report about the quality of rain gauges that Matxitxako (C019) rain gauge underestimates precipitation, mainly due to wind exposure. Figure 6 shows a return period fitting diagnostic plot for precipitation duration of 1440 minutes at this location. Note that even though diagnostic fitting tests do not reject either the local or the spatial fitting with p-values equal to 0.21 and 0.24, respectively. This is probably due to the uncertainty associated with the short record length, return periods related to a particular precipitation amount given by the spatial fitting are significantly lower than the local equivalents, i.e. the spatial model makes the model less prone to return period underestimation due to instrumental bias. This correction is induced by the spatial coherence given by the model.

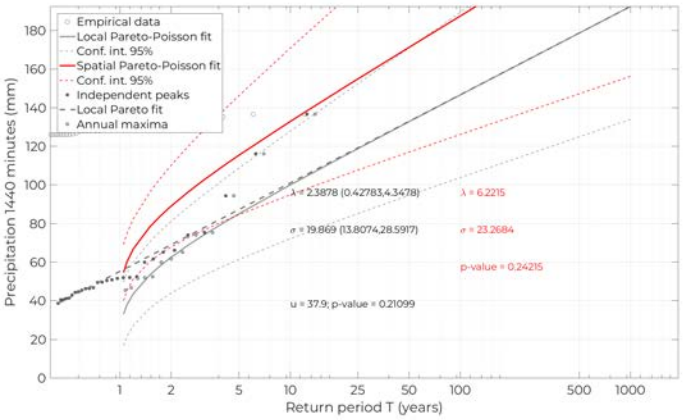

Fig. 6 Fitted return periods for 1440 minutes timescale at Matxitxako (C019) rain gauge.

Another example about the robustness of the spatial model against instrumental bias corresponds to the fitting at Zaldiaran (Repetidor) rain gauge, where in addition to underestimation induced by wind exposure the presence of physical obstacles (branch trees) is also confirmed. Note in Figure 7 how the spatial model pushes up return period estimates clearly above local fitting estimates and empirical data.

3. **Being robust with respect the existence of gaps in the record, enabling not to discard records of incomplete years with a high percentage of gaps in the series.** This feature is taken into consideration due to the fact that exceedances over threshold are chosen instead of annual maxima, and exceedances mostly occur uniformly distributed during the year.
4. **Make it robust with respect to the length of the series.** There is no doubt that the longer the record, the lower the uncertainty in return period estimations. It would be convenient to have a method that gives

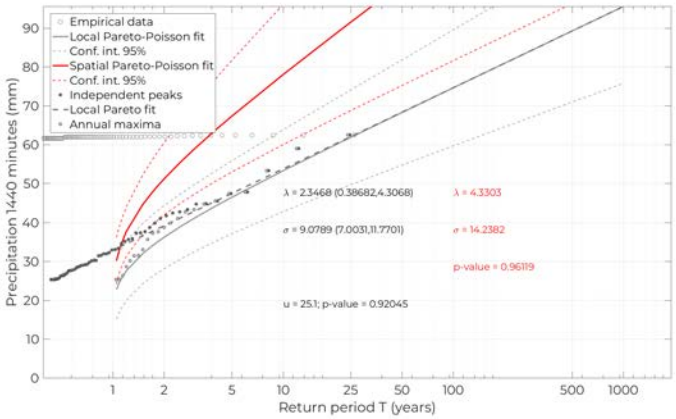

Fig. 7 Fitted return periods for 1440 minutes timescale at Zaldiaran (Repetidor) (C070) rain gauge.

more weight to long records than to short ones, without the need to discard short ones from the analysis. In this particular case, the spatial model considered allows to make a unique fitting process where the longer the record the higher the influence according to expression (11).

5. **Allowing coherent spatial interpolation/extrapolation, i.e. taking into account the influence of orographic factors such as elevation, distance from shoreline, blockages, exposures, curvatures, etc.** In this particular case, the spatial coherence and the influence of those factors are taken into consideration though covariates related to GEV parameters from daily gridded data set. If we compare the digital elevation model in Figure 4 with respect to 100 years return period estimates for different timescales, such as 10 and 1440 minutes shown in Figures 8(a) and 8(b) respectively, a clear influence of orographic factors is observed.

Previous results show the performance of the method when there are data issues, but there are many locations where both local and spatial fits are very similar, which increase the confidence in the return period estimates at those locations, and the confidence in the proposed model. Figures 9(a) and 9(b) shown return period estimates at Altzola and Sarria rain gauges using local and spatial analysis. In both cases the resulting return period estimates are very similar, which shows that when the data quality at rain gauge locations is appropriate, both local and spatial analyses provide consistent results. This behaviour has been observed at many locations and with different timescales.

3.3 Leave-one-out cross validation

We have also performed a leave-one-out cross validation procedure to check the interpolation capabilities associated with the spatial model. Figure 10 shows the scatter plot associated with location and scale spatial fitted parameters for

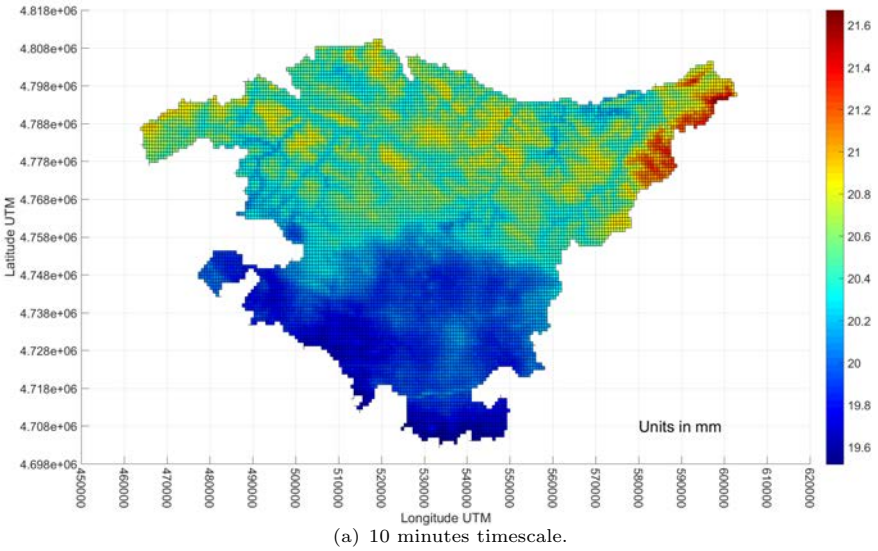

(a) 10 minutes timescale.

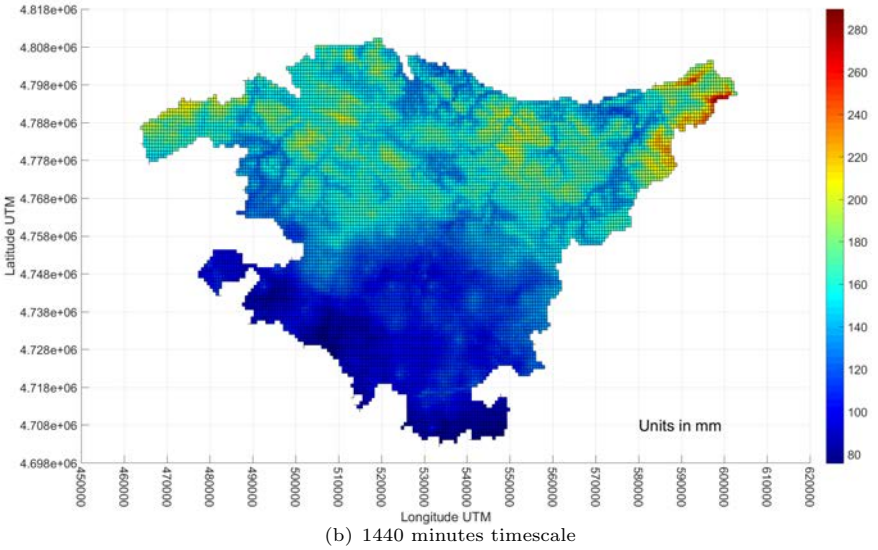

(b) 1440 minutes timescale

Fig. 8 100 year return period estimates in mm over the 1 km spatial resolution grid.

a) all rain gauges data (abscisas axis) and b) leave-one-out process (ordinates axis). Results show that the estimated parameters between both approaches are indistinguishable, with points following almost a perfect straight diagonal. However, numerical results change from the third decimal. We only show results associated with 10 minutes timescale, but these results are analogous for the rest of timescales and prove the robustness of the proposed method,

which makes return period estimations less prone to bias due to difficulties in data gathering.

3.4 Model validation using a large high quality rain gauge

The longest record used in the analysis corresponds to Lastur (LAST) rain gauge with 31.875 years, which is relatively short for an extreme value analysis. In order to check the coherence of return period estimations given by the spatial model, we have at our disposal a long record of 85.55 years at San Sebastián-Igeldo (1024E) rain gauge, with UTM coordinates (577907, 4795405) and 259 m heigh, which was not used during the fitting process. Fortunately, we also have another rain gauge (Igeldo DFG) which contains a record length of 24.371 years at 250 m altitude and very close (less than 500 m) to Sebastián-Igeldo (1024E) rain gauge. This proximity allows us to compare results obtained using the proposed method and the local analysis, with the shorter record, with respect to the longest additional record, i.e. validate results.

Note that both local and spatial return periods at Igeldo DFG rain gauge are very similar (see Figure 11(a)), and in both cases we can not reject the null hypothesis that data comes from both distributions. On the other hand, the spatial model particularized at Sebastián-Igeldo (1024E) rain gauge location is shown in Figure 11(b). In this particular case, instrumental data is slightly above the spatial return period fitted model, which runs almost parallel to the local fitted model. However, we can not reject the null hypothesis that the data at this location comes from the fitted spatial model. In fact, the spatial model is between local model confidence bands. This result indicates that even though we are using relatively short records, mostly below 30 years, the use of longer series of spatial gridded data products allows getting consistent results.

3.5 Model validation comparing with dimensionless IDF curves

The ratio between the precipitation of a given duration and that of 24 hours is an indication of the degree of torrential rains in a region. In rain gauges with a significant record length, it is an observed fact that these proportions remain approximately constant and independent of the return period considered. This feature is widely used in practice especially when no many records of timescales lower than 6 hours are available. In those cases, we use those records to compute those relations and use them all over the study area.

However, if we make this analysis at all rain gauges locations using return periods associated with local and spatial analysis, we get results shown in Figures 12(a) and 12(b), respectively. Note that dashed lines related to “valle”, “monte” and “costa” are the curves used in previous reports to make IDF analyses. Dots corresponds to values related to specific rain gauges and return periods, while we have fitted power curves to those data in an attempt to get representative expressions for each return period considered. Note that data

dispersion for the local case is large, clearly contradicting the initial hypothesis that proportions remain approximately constant. The spatial analysis also has dispersion around fitted curves, but considerably lower than the local case. In addition, fitted power curves are almost independent from return period, i.e. spatial analysis seems to be more consistent with this hypothesis of constant proportions.

3.6 Cramer-von Mises vs Anderson-Darling tests

We performed to validation tests to check the null hypothesis that exceedances and annual maxima follow the fitted distributions respectively. In particular, we used the modification of the Cramer-von Mises and Anderson-Darling distributional fitting tests proposed by Chen and Balakrishnan (1995), which work with the GPD and GEV distributions and where user can provide the distribution parameters. However, we only show the Cramer-von Mises test results. The reason is that very similar results are obtained in both cases, as shown in Figure 13. The figure shows the scatter plot of p-values related to local and spatial analyses associated with Cramer-von Mises test statistic (left panel) and Anderson-Darling test statistic (right panel). Note that local and spatial analyses present very similar diagnostics, with p-values slightly changing around the diagonal. If we compare the scattet plots for both tests, they are very similar in terms of dispersion and variation range, which justifies why we only present results associated with Cramer-von Mises test.

3.7 Further discussion on the type of tail obtained from the analyses

Koutsoyiannis et al (1998); Koutsoyiannis (1998a,b); Papalexiou and Koutsoyiannis (2013) have done an extensive work in comparing and concluding in the best GEV type for the rainfall extremes. In those studies it is clear that the rainfall extremes follow a GEV type II distribution (with shape parameter values converging at $0.1 - 0.15$), and this type of GEV should be preferred mainly for high return periods ($T > 50$ years) because the Gumbel distribution is very conservative and clearly underestimates the rainfall extremes. In those studies, it is pointed out that because of the short time series available ($20 - 30$ years available) for the extreme analysis, the Gumbel distribution is falsely chosen as the best fit. Even though the type 1 error is small and test statistics accept Gumbel as a suitable distribution, the type 2 error is quite large (up to 80%). Thus, even though here the test statistics are accepting and fitting Gumbel distribution, 30 years (at best case) of observation data may hide the true distribution and cause a severe underestimation of the IDF curves especially at high return periods.

In our analysis most of the fitting models correspond to Gumbel, which contradicts Koutsoyiannis and coauthors findings. The reason is that we compute and show confidence bands for return periods. It is well-known that uncertainty associated with long return period estimation, especially when

dealing with short records, is usually large. We rather trust the proper statistical analysis and take into consideration the uncertainty when using the information about return period estimates. Let consider the example shown in Figure 11(b), where the spatial model is validated with a very long record (≈85 years); in this particular case, even the local analysis using the Pareto-Poisson model with this long record returns the Gumbel distribution as best fit, disregarding the hypothesis that the shape parameter is statistically different from zero. In our opinion, engineers should work with not only the point estimates of return periods but their uncertainties as well. This will avoid underestimation of return periods and forcing the statistical models to follow a predefined tail without further extreme value analysis statistical considerations.

4 Conclusions

In this work a new methodological framework for the spatial analysis of extreme rainfall intensities at different time scales has been described and tested over the Basque Country. The method presents the following positive features:

1. It is aligned with the current trend of climate data availability in which observational and gridded datasets coexist, the former with high temporal frequency and the latest describing the spatial variability and orographic dependencies of the different precipitation regimes over a particular region. In this sense, the proposed framework can be easily adapted to other regions and applied to make a coherent and robust spatial analysis of extreme intensity rainfall for different timescales, including IDF curves generation.
2. The proposed approach has proved to be robust with respect to the main issues coming from observational datasets, which includes outliers, systematic biases, missing data and short length time series.
3. Dependencies induced by orographic factors, such as elevation, distance from shoreline, blockages, exposures, curvatures, etc. are properly modelled through the use of covariates coming from the high-resolution gridded dataset.

The methodology has been used to obtain the IDF curves over the Basque Country and tested against local observations, including Sebastián-Igeldo (1024E) rain gauge record, the longest record available, which was not used during the calibration process. The method shows the statistical coherence between the estimated local and spatial return periods, with the latest falling within the confidence intervals of the former.

Finally, the positive features of the method and its robustness might justify the effort of developing specific high resolution daily precipitation gridded data sets prior making any extreme value analysis of intensity rainfall.

Acknowledgments. This research is part of the project "Development of IDF curves in the Basque Country", financed by the Basque Water

Agency (URA). In addition, we acknowledge funding from the Projects INDECIS (Grant 690462) and WATExR (https://watexr.eu/), part of European Research Area for Climate Services Consortium (ERA4CS) with co-funding by the European Union. WATExR was partially funded by MINECO-AEI (ES) through the project PCIN-2017-092.

References

Akaike H (1973) Information theory and an extension of the maximum likelihood principle. In: Petrov BN, Csáki F (eds) Proceedings 2nd International Symposium on Information Theory. Akadémia Kiadó, Budapest, pp 267–281

Artetxe A, del Hierro O, Herrera S (2019) Escenarios de cambio climático de alta resolución para el país vasco. Fase II: Datos diarios con metodologías de corrección de sesgo. Report (in spanish), Ihobe, Ingurumen Jarduketarako Sozietate Publikoa (Sociedad Pública de Gestión Ambiental), Ihobe, Sociedad Pública de Gestión Ambiental. Departamento de Medio Ambiente, Planificación Territorial y Vivienda (Gobierno Vasco) Alda. de Urquijo n.o 36-6.a (Plaza Bizkaia) 48011 Bilbao

Atkinson M, Lloyd C (1998) Mapping precipitation in switzerland with ordinary and indicator kriging. Journal of Geographic Information and Decision Analysis 2:72–86.

Bedia J, Herrera S, Gutiérrez J (2013) Dangers of using global bioclimatic datasets for ecological niche modeling. limitations for future climate projections. Global and Planetary Change 107:1–12. https://doi.org/10.1016/j.gloplacha.2013.04.005

Belo-Pereira M, Dutra E, Viterbo P (2011) Evaluation of global precipitation data sets over the iberian peninsula. Journal of Geophysical Research: Atmospheres 116(D20). https://doi.org/doi.org/10.1029/2010JD015481

Beran MA, Nozdryn-Plotnicki MK (1977) Estimation of low return period floods. Bull Int Ass Hydrol Sci 22(2):275–282

Biau G, Zorita E, Von Storch H, et al (1999) Estimation of precipitation by kriging in the eof space of the sea level pressure field. Journal of Climate 12(4):1070–1085. https://doi.org/10.1175/1520-0442(1999)012⟨1070:EOPBKI⟩2.0.CO;2

Box GEP, Pierce DA (1970) Distribution of residual autocorrelations in autoregressive-integrated moving average time series models. Journal of the American Statistical Association 65(332):1509–1526. https://doi.org/10.1080/01621459.1970.10481180

Brockwell PJ, Davis RA (1991) Time series: Theory and methods, 2nd edn. Springer-Verlag, New York, NY

Brown SJ, Caesar J, Ferro AT (2008) Global changes in extreme daily temperature since 1950. Journal of Geophysical Research 113. D05115, doi:10.1029/2006JD008091

Carter DJT, Challenor PG (1981) Estimating return values of environmental variables. Quart J Roy Meteor Soc 107:259–266

Castillo E (1988) Extreme Value Theory in Engineering. Academic Press, New York

Castillo E, Hadi AS, Balakrishnan N, et al (2005) Extreme Value and Related Models in Engineering and Science Applications. John Wiley & Sons, New York

Castillo E, Castillo C, Mínguez R (2008) Use of extreme value theory in engineering design. In: Martorel CS. Guedes Solares, Barnett J (eds) Proceedings of the European Safety and Reliability Conference 2008 (ESREL 2008), Safety, Reliability and Risk Analysis: Theory, Methods and Applications, vol 3. Taylor & Francis Group, Valencia, p 2473–2488

Chen G, Balakrishnan N (1995) A general purpose approximate goodness-of-fit test. Journal of Quality Technology 27(2):154–161. https://doi.org/10.1080/00224065.1995.11979578

Coleman TF, Li Y (1994) On the convergence of reflective newton methods for large-scale nonlinear minimization subject to bounds. Mathematical Programming 67(2):189–224

Coleman TF, Li Y (1996) An interior, trust region approach for nonlinear minimization subject to bounds. SIAM Journal on Optimization 6:418–445

Coles S (2001) An introduction to statistical modeling of extreme values. Springer Series in Statistics

Davidson AC, Smith RL (1990) Models for exceedances over high thresholds. Journal of the Royal Statistical Society Series B (Methodological) 52(3):393–442

Dirk N. Karger D, Lange S, Hari C, et al (2021) Chelsa-w5e5 v1.1: W5e5 v1.0 downscaled with chelsa v2.0. Isimip repository, Inter-Sectoral Impact Model Intercomparison Project, https://doi.org/doi.org/10.48364/ISIMIP.836809.1

Fisher RA, Tippett LHC (1928) Limiting forms of the frequency distributions of the largest or smallest member of a sample. Journal of Coastal Research 24:180–190

Frei C, Schär C (1998) A precipitation climatology of the alps from high-resolution rain-gauge observations. International Journal of Climatology 18(8):873–900. https://doi.org/doi.org/10.1002/(SICI)1097-0088(19980630)18:8⟨873::AID-JOC255⟩3.0.CO;2-9

Galambos J (1987) The Asymptotic Theory of Extreme Order Statistics. Robert E. Krieger Publishing Company, Malabar, Florida

George EI, Foster DP (1994) The risk inflation criterion for multiple regression. Ann Statist 22:1947–1975

Gesch D, Verdin K, Greenlee S (1999) New land surface digital elevation model covers the earth. Eos 80(6):69–70. https://doi.org/10.1029/99EO00050

Grimaldi S, Kao SC, Castellarin A, et al (2011) 2.18 - statistical hydrology. In: Wilderer P (ed) Treatise on Water Science. Elsevier, Oxford, p 479 – 517, https://doi.org/doi.org/10.1016/B978-0-444-53199-5.00046-4

Haylock M, Hofstra N, Klein Tank A, et al (2008) A european daily high-resolution gridded data set of surface temperature and precipitation for 1950-2006. Journal of Geophysical Research Atmospheres 113(20). https://doi.org/10.1029/2008JD010201

Hengl T, Heuvelink G, Rossiter D (2007) About regression-kriging: From equations to case studies. Computers and Geosciences 33(10):1301–1315. https://doi.org/10.1016/j.cageo.2007.05.001

Herrera S, Gutiérrez JM, Ancell R, et al (2012) Development and analysis of a 50-year high-resolution daily gridded precipitation dataset over spain (spain02). International Journal of Climatology 32(1):74–85. https://doi.org/doi.org/10.1002/joc.2256

Herrera S, Cardoso RM, Soares PM, et al (2019a) Iberia01: a new gridded dataset of daily precipitation and temperatures over iberia. Earth System Science Data 11(4):1947–1956. https://doi.org/10.5194/essd-11-1947-2019

Herrera S, Kotlarski S, Soares P, et al (2019b) Uncertainty in gridded precipitation products: Influence of station density, interpolation method and grid resolution. International Journal of Climatology 39(9):3717–3729. https://doi.org/10.1002/joc.5878

Hofstra N, New M, McSweeney C (2010) The influence of interpolation and station network density on the distributions and trends of climate variables

in gridded daily data. Climate Dynamics 35(5):841–858. https://doi.org/10.1007/s00382-009-0698-1

Hurvich CM, Tsai CL (1989) Regression and time series model selection in small samples. Biometrika 76:297–307

Izaguirre C, Méndez FJ, Menéndez M, et al (2010) Extreme wave climate variability in Southern Europe using satellite data. Journal of Geophysical Research 115(C04009):1–13. https://doi.org/10.1029/2009JC005802

Izaguirre C, Menéndez M, Camus P, et al (2012) Exploring the interannual variability of extreme wave climate in the northeast atlantic ocean. Ocean Modelling 59–60:31–40. https://doi.org/http://dx.doi.org/10.1016/j.ocemod.2012.09.007

Katz RW, Parlange MB, Naveau P (2002) Statistics of extremes in hydrology. Advanced Water Resources 25:1287–1304

Klein Tank AMG, Wijngaard JB, Können GP, et al (2002) Daily dataset of 20th-century surface air temperature and precipitation series for the european climate assessment. International Journal of Climatology 22(12):1441–1453. https://doi.org/doi.org/10.1002/joc.773

Klok EJ, Klein Tank AMG (2009) Updated and extended european dataset of daily climate observations. International Journal of Climatology 29(8):1182–1191. https://doi.org/doi.org/10.1002/joc.1779

Koutsoyiannis D (1998a) Statistics of extremes and estimation of extreme rainfall: I. Theoretical investigation. Hydrological Sciences Journal 49(4):590. https://doi.org/10.1623/hysj.49.4.575.54430

Koutsoyiannis D (1998b) Statistics of extremes and estimation of extreme rainfall: II. Empirical investigation of long rainfall records. Hydrological Sciences Journal 49(4):591–610. https://doi.org/10.1623/hysj.49.4.591.54424

Koutsoyiannis D, Kozonis D, Manetas A (1998) A mathematical framework for studying rainfall intensity-duration-frequency relationships. Journal of Hydrology 206(1–2):118–135

Lange S (2016) Earth2observe, wfdei and era-interim data merged and bias-corrected for isimip (ewembi). Report gfz data services, Potsdam Institute for Climate Impact Research. https://doi.org/10.5880/pik.2016.004

Lange S (2019) Earth2observe, wfdei and era-interim data merged and bias-corrected for isimip (ewembi) v.1.1. Report gfz data services, Potsdam Institute for Climate Impact Research. https://doi.org/10.5880/pik.2019.004

Leadbetter M, Lindgren G, Rootzén H (1983) Extremes and related properties of random sequences and processes. Springer-Verlag, New York

Lehmann EL, Casella G (1998) Theory of Point Estimation, 2nd edn. Springer Text in Statistics, Springer, New York

Ljung GM, Box GEP (1978) On a measure of lack of fit in time series models. Biometrika 65(2):297–303. https://doi.org/10.1093/biomet/65.2.297

MATLAB (2018) 9.7.0.1190202 (R2019b). The MathWorks Inc., Natick, Massachusetts

Méndez FJ, Menéndez M, Luceño A, et al (2006) Estimation of the long term variability of extreme significant wave height using a time-dependent POT model. J of Geophys Res 111. https://doi.org/10.1029/2005JC003344

Méndez FJ, Menéndez M, Luceño A, et al (2007) Analyzing monthly extreme sea levels with a time-dependent GEV model. J Atmos Ocean Technol 24:894–911

Menéndez M, Méndez FJ, Izaguirre C, et al (2009) The influence of seasonality on estimating return values of significant wave height. Coastal Engineering 56(3):211–219

Mínguez R, Del Jésus F (2015) Revisited mixed extreme wave climate model for reanalysis databases. Stochastic Environmental Research and Risk Assessment 29(7):1851–1856. https://doi.org/10.1007/s00477-014-0937-9

Mínguez R, Méndez FJ, Izaguirre C, et al (2010) Pseudo-optimal parameter selection of non-stationary generalized extreme value models for environmental variables. Environmental Modelling & Software 25:1592–1607. https://doi.org/10.1016/j.envsoft.2010.05.008

Mínguez R, Tomás A, Méndez FJ, et al (2013) Mixed extreme wave climate model for reanalysis databases. Stochastic Environmental Research and Risk Assessment 27:757–768. https://doi.org/10.1007/s00477-012-0604-y

Morton ID, Bowers J, Mould G (1997) Estimating return period wave heights and wind speeds using a seasonal point process model. Coastal Engineering 31:305–326

Northrop P (2004) Likelihood-based approaches to flood frequency estimation. Journal of Hydrology 292:96–113

Oehlert GW (1992) A note on the Delta Method. The American Statistician 46(1):27–29

Tiago de Oliveira J (1958) Extremal distributions. Revista de la Facultade de Ciencias 7(2A):215–227

Papalexiou SM, Koutsoyiannis D (2013) Battle of extreme value distributions: A global survey on extreme daily rainfall. Water Resour Res 49:187–201. https://doi.org/10.1029/2012WR012557

Salas JD, L. AM, Papalexiou SM, et al (2020) PMP and climate variability and change: A review. J Hydrol Eng 25(12):03120,002

Schwarz G (1978) Estimating the dimension of a model. Ann Statist 6:461–464

Smith RL (2001) Environmental Statistics. Department of Statistics, University of North Carolina

Smith RL, Shively TS (1995) A point process approach to modeling trends in tropospheric ozone. Atmospheric Environmental 29:3489–3499

Thornton M, Shrestha R, Wei Y, et al (2020) Daymet: Daily surface weather data on a 1-km grid for north america, version 4. https://doi.org/10.3334/ORNLDAAC/1840

Yan L, Xiong L, Jiang C, et al (2021) Updating intensity–duration–frequency curves for urban infrastructure design under a changing environment. WIREs Water 8(3):e1519. https://doi.org/10.1002/wat2.1519

Yatagai A, Xie P, Alpert P (2007) Development of a daily gridded precipitation data set for the middle east. Advances in Geosciences 12:165–170. https://doi.org/10.5194/adgeo-12-165-2008

Appendix A Information associated with rain gauges

For this study, we have at our disposal the following information about rain gauges:

1. Name of the rain gauge, code and watershed to which it belongs.
2. UTM coordinates and the elevation at which they are located.
3. Start date of the record.
4. End date of the record.
5. Temporal frequency of the records.
6. Total number of data available and number of data without information (*not a number*).
7. Number of years of record length taking into account the sampling frequency and the number of data available. Note that the vast majority of records are above 5 years long, and that is the minimum length criterion

that we have used in this analysis. Good practice rules advise against conducting extreme value analysis with less than 5 years of data, and for this reason they are discarded.

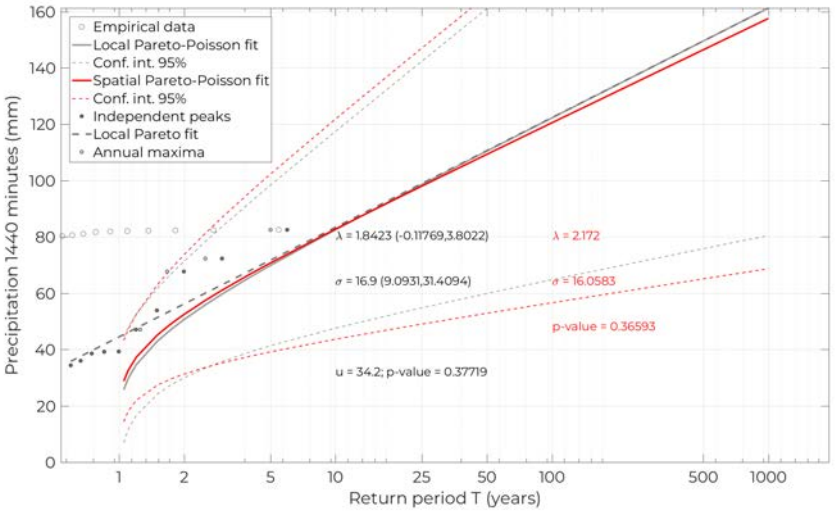

(a) Igeldo DFG rain gauge.

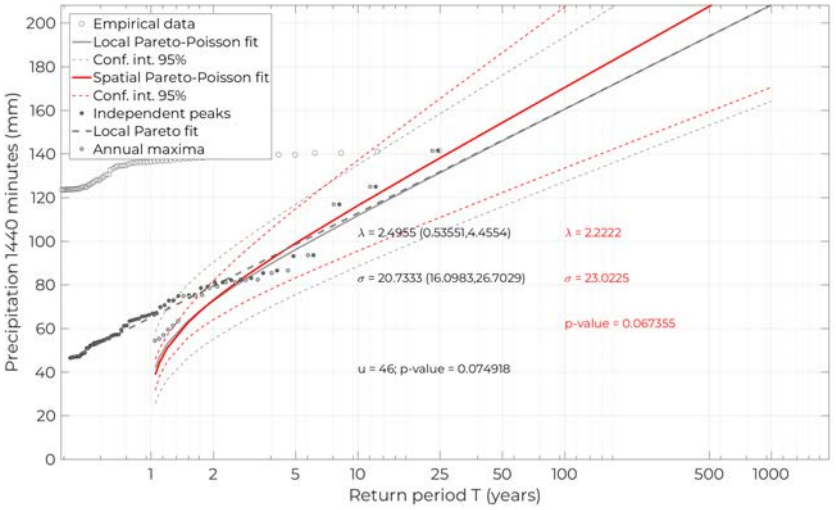

(b) Altzola rain gauge.

Fig. 9 Estimated return periods for 1440 minutes timescale at Altzola and Sarria rain gauges using: i) local analysis and ii) spatial analysis .

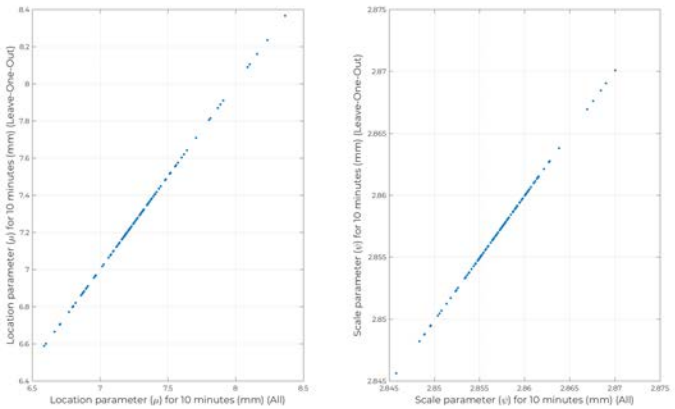

Fig. 10 Scatter plot associated with location and scale spatial fitted parameters for a) all rain gauges data (abscisas axis) and b) leave-one-out process (ordinates axis).

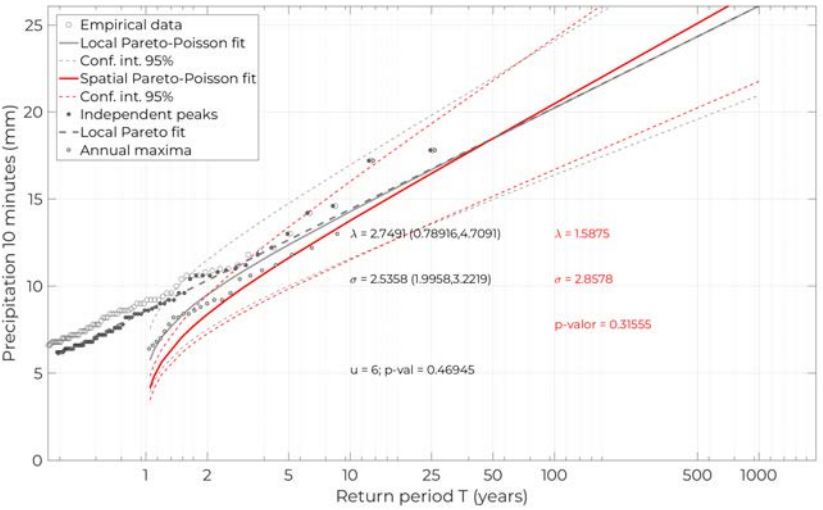

(a) Igeldo DFG rain gauge.

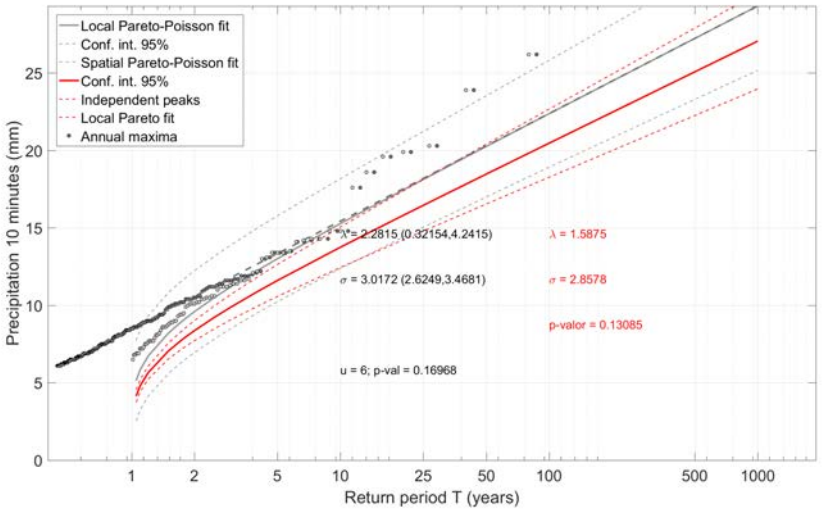

(b) Sebastián-Igeldo (1024E) rain gauge.

Fig. 11 Estimated return periods for 10 minutes timescale at two close locations in San Sebastián using: i) local analysis with a relatively short record (24.371 years), ii) spatial analysis using all short records, and iii) local analysis using long record (85.55 years).

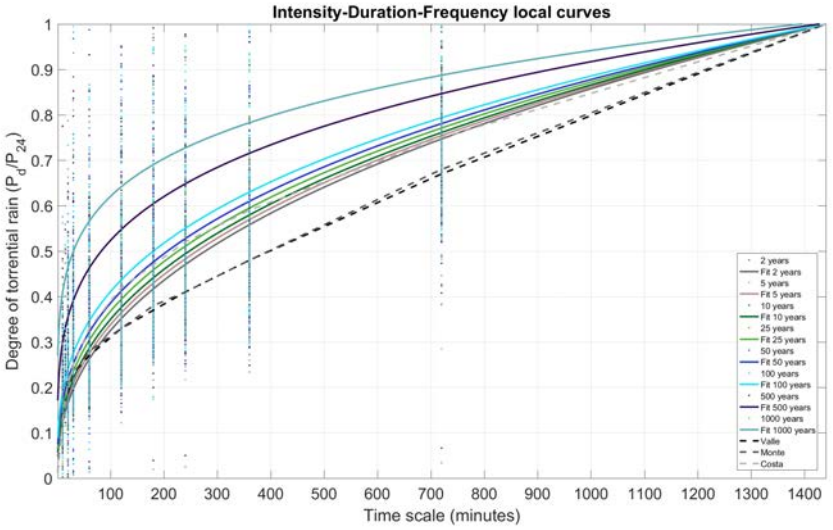

(a) Local analysis.

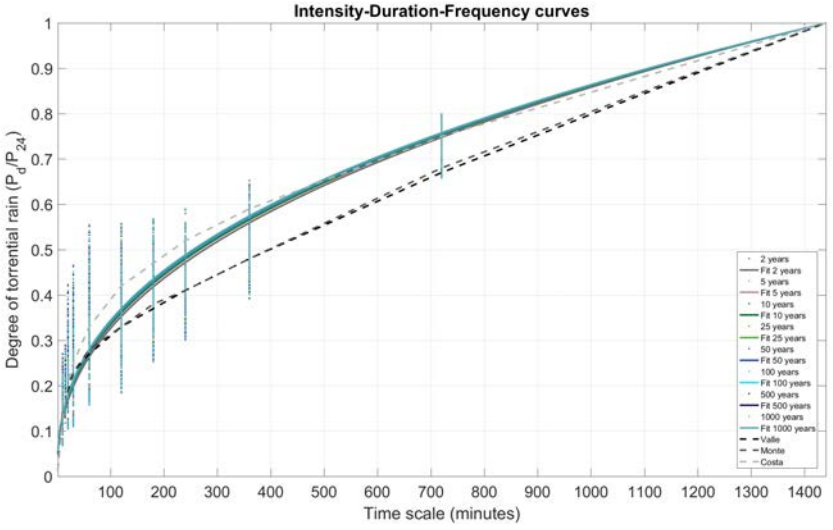

(b) Spatial analysis.

Fig. 12 Dimensionless IDF curves using extreme value analysis.

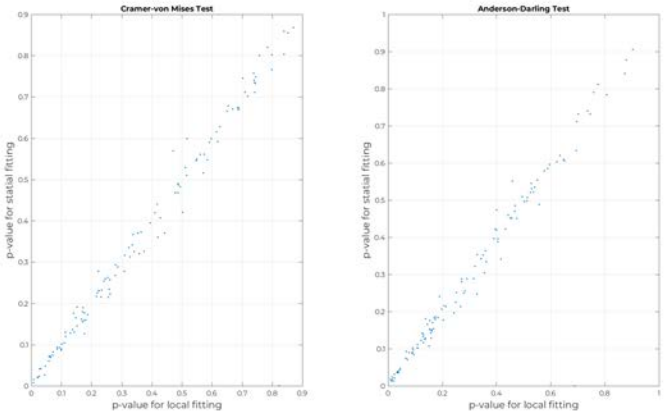

Fig. 13 Scatter plot related to p-values for local and spatial analyses: a) Cramer-von Mises test statistic (left panel) and b) Anderson-Darling test statistic (right panel).

Table A1: Rain gauge data available.

Name	Code	Watershed	UTMX	UTMY	Altitude(m)	From	To	Frequency	nº data	nº NaN	Years
Ilarduia	C068	Arakil	558297.0	4747064	596	20/02/2015 00:00	31/10/2020 23:50	10 minutes	299664	208	5.694
Urdalur	E074	Arakil	562559.0	4751876	652	26/10/2005 22:00	14/07/2019 21:45	15 minutes	480864	32605	12.784
Berriatua	C0BE	Artibai	542501.0	4794747	25	01/11/2001 00:00	31/10/2020 23:50	10 minutes	999360	2059	18.962
Iruzubieta	C0BD	Artibai	538484.0	4789312	110	26/01/2012 12:50	31/10/2020 23:50	10 minutes	461011	147	8.762
Beluntza	C025	Baias	508688.0	4756573	687	21/02/2008 02:30	12/12/2013 08:30	10 minutes	305461	350	5.801
Ormijana	P070	Baias	505098.0	4741843	645	12/04/2009 22:00	14/07/2019 21:45	15 minutes	359520	11019	9.939
Sarria	C0A0	Baias	513848.0	4758370	655	19/05/2011 13:50	31/10/2020 23:50	10 minutes	497293	137	9.452
Subijana (Peaje)	C049	Baias	508725.0	4740572	537	01/10/1992 00:00	31/10/2020 23:50	10 minutes	1477152	6544	27.960
Behobia	C084	Bidasoa	600414.0	4799749	5	21/05/2013 08:00	31/10/2020 23:50	10 minutes	391776	267	7.444
Endara	F1Z1	Bidasoa	599379.0	4791335	273	28/11/1996 12:50	30/09/2020 23:50	10 minutes	1253875	150280	20.982
Endara	F1W1	Bidasoa	599379.0	4791335	273	28/11/1996 12:50	30/09/2020 23:50	10 minutes	1253875	307897	17.986
Endara antigua	ENDA	Bidasoa	599799.0	4792576	200	28/10/1989 00:00	24/10/1996 11:30	10 minutes	367702	21549	6.581
Mungia (DAEM)	C057	Butroe	512460.0	4800977	22	06/12/1992 00:00	31/10/2020 23:50	10 minutes	1467648	27733	27.377
Aixola	C0D3	Deba	540536.0	4777916	349	10/10/1989 00:00	31/10/2020 23:50	10 minutes	1633680	64209	29.840
Altzola	C078	Deba	548867.0	4787631	17	10/12/1995 00:00	31/10/2020 23:50	10 minutes	1309392	2583	24.846
Arantzazu Pluviometro	ARAN	Deba	547386.0	4759382	600	13/01/1998 12:00	30/09/2020 23:50	10 minutes	1194696	71626	21.353
Araotz	ARAO	Deba	543354.0	4760985	726	03/03/1987 00:00	30/09/2020 23:50	10 minutes	1766304	584693	22.466
Arrasate	C023	Deba	541311.0	4768691	318	22/10/1998 00:00	31/10/2020 23:50	10 minutes	1158624	2078	21.989
Eitzaga	C075	Deba	540525.0	4780289	270	06/06/2011 10:40	31/12/2019 23:50	10 minutes	450800	11	8.571
Elosua	ELOS	Deba	551032.0	4775383	726	01/10/1999 00:00	30/09/2020 23:50	10 minutes	1104624	38901	20.262
Lastur Pluviometro	LAST	Deba	554285.0	4786830	546	26/11/1985 00:00	30/09/2020 23:50	10 minutes	1832832	156339	31.875
Mendaro	MEND	Deba	550609.0	4788574	45	01/10/1989 00:00	30/09/2020 23:50	10 minutes	1630512	45902	30.128
Oñati	C0D1	Deba	545798.0	4767651	195	31/10/1997 00:00	31/10/2020 23:50	10 minutes	1209888	7454	22.862
San Prudentzio	C0D2	Deba	544970.0	4769996	169	08/03/1997 00:00	31/10/2020 23:50	10 minutes	1244016	2256	23.609
Urkulu	C0D0	Deba	542991.0	4762167	340	01/10/1989 00:00	31/10/2020 23:50	10 minutes	1634976	24924	30.612
Bollegas	R005	Ebro	489094.0	4735889	1095	31/12/2004 23:00	14/07/2019 21:45	15 minutes	509564	3414	14.435
Moreda	C031	Ebro	548437.0	4708613	490	28/12/2012 11:30	31/10/2020 23:50	10 minutes	412491	4	7.843
Paganos	C060	Ebro	532794.0	4711871	577	06/02/2004 10:40	31/10/2020 23:50	10 minutes	880208	1332	16.710
Sobron (embalse)	E005	Ebro	491819.0	4735037	513	30/09/1997 22:00	14/07/2019 21:45	15 minutes	763872	19171	21.238
Iturrieta (Granja)	C024	Ega	553515.0	4738088	987	29/10/1998 00:00	31/10/2020 23:50	10 minutes	1157616	31971	21.402
Kanpezu	C00A	Ega	553957.0	4724980	550	19/05/2015 12:10	31/10/2020 23:50	10 minutes	286919	22	5.455
Lagran	P008	Ega	534110.0	4719089	750	30/09/1997 22:00	14/07/2019 21:45	15 minutes	763872	10928	21.473
Navarrete	C041	Ega	539067.0	4720514	689	26/04/1992 00:00	31/10/2020 23:50	10 minutes	1499904	13440	28.262
Roitegi	C021	Ega	551450.0	4736772	980	12/03/2008 08:10	26/05/2014 23:50	10 minutes	326399	3005	6.149
San Vicente de Arana	P009	Ega	552301.0	4731749	800	30/09/1997 22:00	14/07/2019 21:45	15 minutes	763872	23016	21.129
Abusu	C0B1	Ibaizabal	507010.0	4788081	23	16/10/1996 00:00	31/10/2020 23:50	10 minutes	1264608	8947	23.874
Altube (Peaje)	C035	Ibaizabal	510768.0	4756856	618	17/01/1999 00:00	31/10/2020 23:50	10 minutes	1146096	8162	21.635
Amorebieta	C079	Ibaizabal	521701.0	4784906	65	07/07/1998 00:00	31/10/2020 23:50	10 minutes	1174032	3159	22.262
Aranguren	C0C1	Ibaizabal	489614.0	4784347	87	10/11/1995 00:00	31/10/2020 23:50	10 minutes	1313712	30659	24.394
Arboleda	C061	Ibaizabal	494527.0	4793551	329	30/06/2004 12:30	31/10/2020 23:50	10 minutes	859317	2364	16.293
Areta	C032	Ibaizabal	505281.0	4776059	122	06/02/2013 00:00	31/10/2020 23:50	10 minutes	406800	11	7.734
Balmaseda	C0C2	Ibaizabal	482208.0	4780281	174	28/05/1994 00:00	31/10/2020 23:50	10 minutes	1390176	21733	26.018
Berna	C0B6	Ibaizabal	526625.0	4781434	92	13/06/1994 00:00	31/10/2020 23:50	10 minutes	1387872	20796	25.992
Derio	C003	Ibaizabal	511885.0	4793192	30	24/05/1996 00:00	31/10/2020 23:50	10 minutes	1285488	18484	24.089
Deusto	C039	Ibaizabal	502602.0	4792076	3	06/11/2001 00:00	31/10/2020 23:50	10 minutes	998640	1460	18.959
Elorrio	C074	Ibaizabal	535914.0	4775188	170	29/09/2000 00:00	31/10/2020 23:50	10 minutes	1056672	1671	20.059
Galindo (CABB)	C038	Ibaizabal	500099.0	4794602	5	13/11/2013 11:10	31/10/2020 23:50	10 minutes	366413	532	6.956
Gardea	C067	Ibaizabal	501592.0	4774734	150	20/08/1995 00:00	31/10/2020 23:50	10 minutes	1325520	29922	24.633
Igorre	C033	Ibaizabal	517579.0	4779317	150	23/03/1999 00:00	31/10/2020 23:50	10 minutes	1136736	4582	21.525
Iurreta	C036	Ibaizabal	530890.0	4780242	170	17/07/2001 00:00	31/10/2020 23:50	10 minutes	1014768	2164	19.252
La Garbea	C045	Ibaizabal	484272.0	4784708	717	11/01/1992 00:00	31/10/2020 23:50	10 minutes	1515168	82649	27.236
Llodio	C027	Ibaizabal	504040.0	4776422	207	06/05/1999 00:00	05/02/2013 23:50	10 minutes	723600	2111	13.718

Continue

Name	Code	Watershed	UTMX	UTMY	Altitude(m)	From	To	Frequency	nº data	nº NaN	Years
Mañaria	C0B7	Ibaizabal	528734.0	4776621	168	03/04/2003 11:30	31/10/2020 23:50	10 minutes	924699	2681	17.530
Ordunte	C059	Ibaizabal	476915.0	4778667	300	30/05/1998 00:00	07/10/2020 10:10	10 minutes	1175966	15944	22.055
Orduña	C072	Ibaizabal	496952.0	4758819	934	19/02/1997 00:00	31/10/2020 23:50	10 minutes	1246464	46836	22.808
Orozko (Altube)	C0B4	Ibaizabal	506869.0	4770195	190	01/07/1994 00:00	31/10/2020 23:50	10 minutes	1385280	57745	25.240
Punta Galea (DAEM)	C042	Ibaizabal	497060.0	4802280	61	26/05/1992 00:00	31/10/2020 23:50	10 minutes	1495584	39000	27.694
Sangroniz	C0B9	Ibaizabal	505608.0	4792707	7	10/02/2012 00:00	31/10/2020 23:50	10 minutes	458928	40	8.725
Saratxo	C051	Ibaizabal	499678.0	4764383	224	21/05/1992 00:00	31/10/2020 23:50	10 minutes	1496304	19938	28.070
Sodupe-Herrerias	C0C4	Ibaizabal	496390.0	4783086	70	18/04/2000 00:00	24/07/2015 23:50	10 minutes	802944	2064	15.227
Sodupe-Kadagua	C0C3	Ibaizabal	496006.0	4783300	80	23/02/2001 00:00	31/10/2020 23:50	10 minutes	1035504	370557	12.643
Urkizu	C0B3	Ibaizabal	518506.0	4781157	75	28/08/1994 00:00	31/10/2020 23:50	10 minutes	1376928	9799	25.993
Zaratamo	C0B2	Ibaizabal	509811.0	4785026	55	01/09/1994 00:00	12/02/2016 23:50	10 minutes	1128240	79522	19.939
Herrera (Puerto)	C048	Inglares	526619.0	4715979	1188	23/07/1992 00:00	31/10/2020 23:50	10 minutes	1487232	38437	27.546
Laurgain	LAUR	Iñurritza	568702.0	4789221	210	21/09/1990 00:00	30/09/2020 23:50	10 minutes	1579392	82352	28.463
Cerroja (balsa)	C065	Karrantza	466929.0	4784134	675	09/03/2001 00:00	31/10/2020 23:50	10 minutes	1033488	19000	19.288
Oiz	C046	Lea	532890.0	4786260	980	18/10/1991 00:00	31/10/2020 23:50	10 minutes	1527408	58812	27.922
Oleta	C0BA	Lea	539813.0	4798978	14	14/11/2001 04:30	31/10/2020 23:50	10 minutes	997461	2076	18.925
Brazuelo	P054	Nela	466474.0	4769272	1074	27/10/1997 23:00	14/07/2019 21:45	15 minutes	761276	51553	20.241
Jaizkibel	C071	Oiartzun	592442.0	4799511	545	01/01/1995 00:00	16/02/2015 23:50	10 minutes	1058688	12370	19.893
Oiartzun	C0F4	Oiartzun	590468.0	4795477	11	05/05/1998 00:00	31/10/2020 23:50	10 minutes	1183104	4430	22.410
Oiartzun DFG	OIAR	Oiartzun	596645.0	4792980	160	12/07/1990 00:00	30/09/2016 10:10	10 minutes	1379150	36405	25.529
Almike (Bermeo)	C069	Oka	521676.0	4806577	106	10/12/2002 00:00	31/10/2020 23:50	10 minutes	941184	6438	17.772
Arteaga	C002	Oka	527675.0	4799209	19	12/01/2011 14:00	31/10/2020 23:50	10 minutes	515580	633	9.791
Matxitxako	C019	Oka	519132.0	4809442	433	01/09/2008 00:00	31/10/2020 23:50	10 minutes	639936	9	12.167
Muxika	C063	Oka	525224.0	4792822	20	20/11/1998 00:00	31/10/2020 23:50	10 minutes	1154448	8384	21.790
Berberana	P005	Omecillo	495327.0	4751712	641	28/03/1997 23:00	14/07/2019 21:45	15 minutes	781724	95000	19.585
Corro	P061	Omecillo	486187.0	4746828	622	04/08/2009 22:00	14/07/2019 21:45	15 minutes	348576	1719	9.892
Espejo	C034	Omecillo	496643.0	4739195	504	23/12/2004 10:40	31/10/2020 23:50	10 minutes	833984	34497	15.201
Agauntza	C0E5	Oria	567033.0	4762906	185	25/09/1996 00:00	31/10/2020 23:50	10 minutes	1267632	9756	23.916
Alegia	C0E9	Oria	572833.0	4772292	95	21/01/1996 00:00	31/10/2020 23:50	10 minutes	1303344	34956	24.116
Ameraun	C052	Oria	585226.0	4776812	285	08/02/1993 00:00	31/10/2020 23:50	10 minutes	1458432	106389	25.706
Amundarain	C0E1	Oria	569178.0	4764663	170	30/11/2001 10:20	31/10/2020 23:50	10 minutes	995122	945	18.902
Araxes	C0E8	Oria	577477.0	4773796	120	30/03/2011 10:30	31/10/2020 23:50	10 minutes	504513	9	9.592
Arriaran DFG	ARRI	Oria	561930.0	4768795	287	02/03/1995 11:00	30/09/2020 23:50	10 minutes	1345614	78694	24.088
Belauntza	C0EA	Oria	577391.0	4776852	105	15/04/1998 00:00	31/10/2020 23:50	10 minutes	1185984	2355	22.504
Berastegi	C026	Oria	582837.0	4774959	379	01/09/2000 00:00	31/10/2020 23:50	10 minutes	1060704	7437	20.026
Bidania	C058	Oria	568736.0	4777177	592	30/04/1993 00:00	31/10/2020 23:50	10 minutes	1446768	21547	27.098
Estanda	C0E7	Oria	563614.0	4766666	200	14/09/1996 00:00	31/10/2020 23:50	10 minutes	1269216	7880	23.982
Ibiur (Estación)	C4Z1	Oria	571731.0	4768129	174	17/09/2009 11:30	30/09/2020 23:50	10 minutes	580539	4816	10.946
Ibiur Pluviometro	IBIU	Oria	571315.0	4769050	270	24/04/1989 11:00	17/10/2013 10:20	10 minutes	1287645	51655	23.500
Lareo	LARE	Oria	572033.0	4758933	745	21/09/1989 17:40	30/09/2020 23:50	10 minutes	1631846	39835	30.269
Lasarte	C0EC	Oria	579430.0	4789116	17	24/03/2000 00:00	31/10/2020 23:50	10 minutes	1083888	4281	20.526
Leitzaran (Andoain)	C077	Oria	579980.0	4784486	94	09/05/1996 00:00	31/10/2020 23:50	10 minutes	1287648	18330	24.133
Ordizia	C043	Oria	566959.0	4766405	243	23/01/1992 00:00	31/10/2020 23:50	10 minutes	1513440	90848	27.048
Troya	TROY	Oria	557370.0	4765545	440	11/08/1994 10:00	30/09/2020 23:50	10 minutes	1374852	87631	24.474
Zaldibia	ZALD	Oria	571320.0	4761615	375	29/11/1989 10:00	30/09/2020 23:50	10 minutes	1621956	84472	29.232
Zarautz (DAEM)	C064	Oria	569358.0	4793558	80	20/02/1993 00:00	31/10/2020 23:50	10 minutes	1456704	23385	27.251
Zegama	C028	Oria	557218.0	4756261	520	11/07/2000 00:00	31/10/2020 23:50	10 minutes	1068192	7139	20.174
Zizurkil	C029	Oria	576218.0	4782109	149	22/07/2000 00:00	31/10/2020 23:50	10 minutes	1066608	3296	20.217
Aitzu	C0DB	Urola	555086.0	4773488	125	31/07/1999 00:00	31/10/2020 23:50	10 minutes	1118016	11059	21.046
Aizarnazabal	C0DD	Urola	561500.0	4789237	25	19/01/1997 00:00	31/10/2020 23:50	10 minutes	1250928	5600	23.677
Barrendiola DFG meteo	BARR	Urola	554107.0	4762714	505	22/09/1989 00:00	30/09/2020 23:50	10 minutes	1631808	105994	29.010
Erdoizta	ERDO	Urola	566743.0	4783605	445	06/12/1990 00:00	30/09/2020 23:50	10 minutes	1568448	78309	28.332
Ibaieder	C0DC	Urola	560477.0	4780317	98	16/02/1996 00:00	31/10/2020 23:50	10 minutes	1299600	14661	24.430

Continue

Name	Code	Watershed	UTMX	UTMY	Altitude(m)	From	To	Frequency	nº data	nº NaN	Years
Matxinbenta	C0DE	Urola	562229.0	4773487	250	08/02/2002 00:00	31/10/2020 23:50	10 minutes	985104	1869	18.694
BARRENDIOLA	B1T1	Urola	553011.0	4761520	550	19/01/2005 14:50	30/09/2020 23:50	10 minutes	825607	14061	15.430
Añarbe (estación)	C080	Urumea	593421.0	4786509	183	28/10/1999 00:00	31/10/2020 23:50	10 minutes	1105200	6368	20.892
Artikutza Eskas	ARTI	Urumea	597144.0	4788113	650	22/10/1999 09:50	30/09/2020 23:50	10 minutes	1101541	4936	20.850
Ereñozu	C0F0	Urumea	586134.0	4788037	26	31/08/1997 00:00	31/10/2020 23:50	10 minutes	1218672	4053	23.093
Igeldo DFG	IGEL	Urumea	577772.0	4795301	250	26/04/1995 10:30	30/09/2020 23:50	10 minutes	1337697	55857	24.371
Miramon	C017	Urumea	583465.0	4793184	113	21/04/2010 12:50	31/10/2020 23:50	10 minutes	553891	647	10.519
Añarbe (estación)	D1Z1	Urumea	593421.0	4786509	183	28/10/1999 00:00	30/09/2020 23:50	10 minutes	1100736	11024	20.719
Abetxuko (CHE)	A317	Zadorra	526418.0	4746786	504	18/08/2014 22:00	14/07/2019 21:45	15 minutes	171936	2390	4.835
Abetxuko (DAEM)	C076	Zadorra	526912.0	4746803	510	05/04/2001 00:00	31/10/2020 23:50	10 minutes	1029600	7221	19.438
Alegria (canal)	C056	Zadorra	538895.0	4743463	545	19/05/1993 00:00	31/10/2020 23:50	10 minutes	1444032	45617	26.588
Alegria Dulantzi	P071	Zadorra	539709.0	4744234	553	16/09/2009 22:00	14/07/2019 21:45	15 minutes	344448	4433	9.697
Arkaute I	C001	Zadorra	530475.0	4744433	517	13/05/1992 00:00	14/02/2017 07:40	10 minutes	1302239	63851	23.545
Barazar	C053	Zadorra	523439.0	4768083	608	06/12/1992 00:00	04/10/2010 07:10	10 minutes	937628	13127	17.577
Etura	C0AA	Zadorra	540549.0	4748262	549	31/01/2012 13:00	31/10/2020 23:50	10 minutes	460290	236	8.747
Gasteiz (Lakua)	C040	Zadorra	525396.0	4745126	546	24/03/1992 00:00	12/12/2013 08:30	10 minutes	1142404	12417	21.484
Gorbea (Embalse)	C044	Zadorra	521589.0	4760576	662	24/10/1992 00:00	31/10/2020 23:50	10 minutes	1473840	54920	26.978
Kapildui	C047	Zadorra	537816.0	4734936	1173	12/11/1991 00:00	31/10/2020 23:50	10 minutes	1523808	210561	24.969
Larrinoa	A221	Zadorra	521862.0	4757556	598	16/03/2009 23:00	14/07/2019 21:45	15 minutes	362108	6103	10.153
Okina	P072	Zadorra	533771.0	4734981	812	03/06/2009 22:00	14/07/2019 21:45	15 minutes	354528	994	10.083
Otxandio (Iberdrola)	C054	Zadorra	527894.0	4765356	556	12/12/1992 00:00	31/10/2020 23:50	10 minutes	1466784	29384	27.329
Ozaeta (Iberdrola)	C055	Zadorra	541375.0	4751070	548	23/02/1993 00:00	31/10/2020 23:50	10 minutes	1456272	100116	25.784
Salvatierra	C030	Zadorra	549355.0	4744857	589	06/02/1999 00:00	31/10/2020 23:50	10 minutes	1143216	5089	21.639
Salvatierra CE	P069	Zadorra	549795.0	4745523	620	10/05/2009 22:00	14/07/2019 21:45	15 minutes	356832	2426	10.107
Trebiño	C020	Zadorra	524447.0	4729536	578	06/11/2007 10:50	31/10/2020 23:50	10 minutes	683071	3672	12.917
Ullibarri (embalse)	E027	Zadorra	531291.0	4753042	545	30/09/1997 22:00	14/07/2019 21:45	15 minutes	763872	21113	21.183
Urkiola	C022	Zadorra	528761.0	4771983	709	12/09/1998 00:00	31/10/2020 23:50	10 minutes	1164384	8406	21.978
Urrunaga	E028	Zadorra	528222.0	4756195	543	30/09/1997 22:00	14/07/2019 21:45	15 minutes	763872	28831	20.963
Zaldiaran (Repetidor)	C070	Zadorra	521556.0	4738051	980	14/07/1994 00:00	31/10/2020 23:50	10 minutes	1383408	42250	25.499
Zambrana	C050	Zadorra	509269.0	4724545	470	15/10/1992 00:00	31/10/2020 23:50	10 minutes	1475136	21027	27.647

Appendix B Estimated parameter confidence intervals

Once the optimal estimates $\hat{\boldsymbol{\theta}}$ that maximize the log-likelihood function (11) is available, the estimated parameters $\hat{\boldsymbol{\theta}}$ correspond to mean values, and assuming that observational errors are normally distributed, the estimated parameter vectors are distributed as follows:

$$\boldsymbol{\theta} \sim N\left(\hat{\boldsymbol{\theta}}, \Sigma_{\boldsymbol{\theta}}\right), \tag{B1}$$

where N denotes the multivariate normal distribution, and $\Sigma_{\boldsymbol{\theta}}$ is the variance-covariance matrix of the parameter estimates. Using the method of maximum likelihood, if $\ell(\cdot)$ is twice differentiable with respect to estimated parameters, and under certain regularity conditions which are often satisfied in practice (Lehmann and Casella (1998)), then the parameter covariance matrix is equal to the inverse of the *Fisher information matrix* ($\boldsymbol{I}_{\boldsymbol{\theta}}$). Assuming that the log-likelihood is approximately quadratic in a neighborhood of the maximum, the *Fisher information matrix* is equal to the Hessian matrix of the log-likelihood functions with the sign changed:

$$\boldsymbol{I}_{\boldsymbol{\theta}} = -\frac{\partial^2 \ell(\boldsymbol{\theta};\, \boldsymbol{x}_{\max})}{\partial^2 \boldsymbol{\theta}}. \tag{B2}$$

The $(1-\alpha)$ confidence interval for each parameter is equal to:

$$\begin{aligned} \theta_j^{\text{up}} &= \hat{\theta}_j + \Phi^{-1}(1-\alpha/2)\hat{\sigma}_j,\ j = 0, 1, \ldots, n_p \\ \theta_j^{\text{lo}} &= \hat{\theta}_j - \Phi^{-1}(1-\alpha/2)\hat{\sigma}_j,\ j = 0, 1, \ldots, n_p, \end{aligned} \tag{B3}$$

where n_p is the number of components of vector $\boldsymbol{\theta}$, $\Phi^{-1}(1-\alpha/2)$ is the standard normal distribution $(1-\alpha/2)$ quantile and $\hat{\sigma}_j$ is the corresponding estimated standard deviation for parameters j (square root of the corresponding diagonal term in $\boldsymbol{\Sigma}_{\boldsymbol{\theta}}$).

Appendix C Quantile confidence intervals

From the practical perspective, the calculation of IDF curves requires computation of quantiles for different return periods (T) (usually in years). These estimated return periods $\hat{x}_T$ correspond to those from solving expression (6) from the fitted distribution at the location of interest.

If we are interested in calculating the confidence bands for estimated quantiles x_{T_k} at location k, and it is known that for large sample sizes the quantile x_{T_k} is asymptotically normal, and thus, the delta method (Oehlert, 1992) can be applied as follows:

$$x_{T_k} \sim N\left(\hat{x}_{T_k}, \nabla_{\boldsymbol{\theta}}^T x_{T_k} \boldsymbol{\Sigma}_{\boldsymbol{\theta}} \nabla_{\boldsymbol{\theta}} x_{T_k}\right), \tag{C4}$$

where $\nabla_{\boldsymbol{\theta}} x_{T_k}$ is the n_p vector of partial derivatives of quantile expressions with respect to $\boldsymbol{\theta}$.

Note that equation (C4) allows obtaining the estimated variance $\hat{\sigma}^2_{x_{T_k}}$ of the quantile, and the confidence intervals then become:

$$\begin{aligned} x^{\text{up}}_{T_k} &= \hat{x}_{T_k} + \sqrt{\frac{n}{n_k}}\Phi^{-1}(1-\alpha/2)\hat{\sigma}_{x_{T_k}}, \\ x^{\text{lo}}_{T_k} &= \hat{x}_{T_k} - \sqrt{\frac{n}{n_k}}\Phi^{-1}(1-\alpha/2)\hat{\sigma}_{x_{T_k}}. \end{aligned} \tag{C5}$$

Note that the proposed method fits parameters using information from all local rain gauges simultaneously $n = \sum_{i=1}^{n_r} n_k$, that is why uncertainty in expression (C5) must be re-scaled to take into consideration the record length at each specific site k. The required derivatives for the return period quantile uncertainty estimation are easily obtained analytically or numerically by finite differences:

$$\frac{\partial z_q}{\partial \gamma} = \frac{z_q(\gamma(1+\epsilon)) - z_q(\gamma(1-\epsilon))}{\epsilon\gamma}, \tag{C6}$$

where γ represents the corresponding parameter and $\epsilon = 10^{-6}$.